Nano-Micro Letters

ISSN 2311-6706
e-ISSN 2150-5551
CN 31-2103/TB

REVIEW

https://doi.org/10.1007/s40820-021-00657-9

Cite as
Nano-Micro Lett.
(2021) 13:134

Received: 27 February 2021
Accepted: 13 April 2021
© The Author(s) 2021

Hydrogen Production via Hydrolysis and Alcoholysis of Light Metal-Based Materials: A Review

Liuzhang Ouyang[1,2] ✉, Jun Jiang[1], Kang Chen[1], Min Zhu[1,2], Zongwen Liu[3,4] ✉

HIGHLIGHTS

- An overview of the recent advances in hydrogen production from light metal-based materials is presented, including hydrolysis of Mg-based alloys and hydrides, hydrolysis of Al-based alloys and hydrides and (catalyzed) hydrolysis/alcoholysis of borohydrides.
- Hydrogen production and storage in a close loop are achieved via hydrolysis and regeneration of borohydrides, demonstrating a promising step toward the large-scale application of chemical hydrogen storage materials in a fuel cell-based hydrogen economy.

ABSTRACT As an environmentally friendly and high-density energy carrier, hydrogen has been recognized as one of the ideal alternatives for fossil fuels. One of the major challenges faced by "hydrogen economy" is the development of efficient, low-cost, safe and selective hydrogen generation from chemical storage materials. In this review, we summarize the recent advances in hydrogen production via hydrolysis and alcoholysis of light-metal-based materials, such as borohydrides, Mg-based and Al-based materials, and the highly efficient regeneration of borohydrides. Unfortunately, most of these hydrolysable materials are still plagued by sluggish kinetics and low hydrogen yield. While a number of strategies including catalysis, alloying, solution modification, and ball milling have been developed to overcome these drawbacks, the high costs required for the "one-pass" utilization of hydrolysis/alcoholysis systems have ultimately made these techniques almost impossible for practical large-scale applications. Therefore, it is imperative to develop low-cost material systems based on abundant resources and effective recycling technologies of spent fuels for efficient transport, production and storage of hydrogen in a fuel cell-based hydrogen economy.

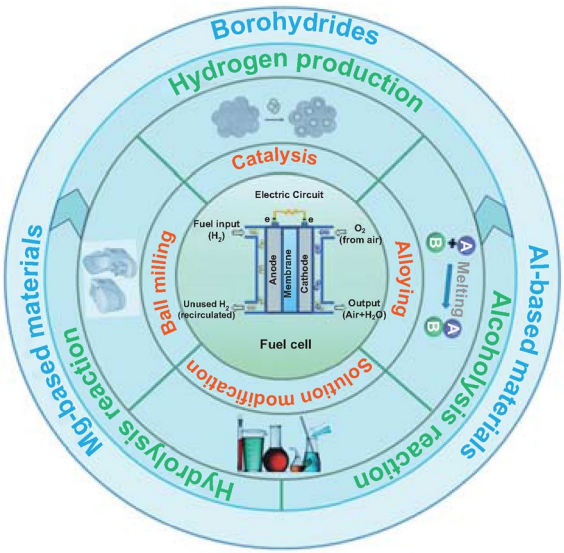

KEYWORDS Hydrolysis; Alcoholysis; Light metal-based materials; Borohydrides; Magnesium; Aluminum; Hydrogen production

✉ Liuzhang Ouyang, meouyang@scut.edu.cn; Zongwen Liu, zongwen.liu@sydney.edu.au
[1] School of Materials Science and Engineering, Guangdong Provincial Key Laboratory of Advanced Energy Storage Materials, South China University of Technology, Guangzhou 510641, People's Republic of China
[2] China-Australia Joint Laboratory for Energy and Environmental Materials, Key Laboratory of Fuel Cell Technology of Guangdong Province, Guangzhou 510641, People's Republic of China
[3] School of Chemical and Biomolecular Engineering, The University of Sydney, Sydney, NSW 2006, Australia
[4] The University of Sydney Nano Institute, The University of Sydney, Sydney, NSW 2006, Australia

Published online: 05 June 2021

Shanghai Jiao Tong University Press

Springer

1 Introduction

Hydrogen, the most abundant content in the universe, has a number of advantages over conventional fuels. It has a high energy density (142 MJ kg^{-1}) and is environmentally friendly. As such, hydrogen energy economy was proposed by Hofman et al. [1] in the early 70s. Encouragingly, the emerging of proton exchange membrane fuel cells (PEMFCs) in the mid-2000s made large-scale hydrogen applications achievable in vehicles or portable electronic devices [2–4]. Particularly, a commercially available car driven by 4 kg of hydrogen fuel can run 400 km with zero carbon oxide emissions [5]. The energy efficiency of this hydrogen 'burnt' process via electrochemically combining with oxygen in fuel cell may reach 70% with less Carnot efficiency loss compared to that in an internal combustion engine [6]. However, the major obstacles for the advent of the hydrogen economy are the absence of efficient strategies for both hydrogen storage and production. Therefore, it is urgent to develop effective solutions to solve these problems from the view of the futuristic aspect of the utilization of hydrogen in stationary, portable and automotive applications [7–9].

As it is known, hydrogen storage methods generally are classified into three types: solid-, liquid- and gas-state. Though ultrahigh-pressure hydrogen and cryogenic-liquid hydrogen technologies are relatively mature and have been applied in various prototype vehicles [10], the hydrogen density barely meets the targets determined by the US Department of Energy (DOE) [11]. For ultrahigh-pressure hydrogen gas, the hydrogen-storage targets of DOE upon onboard hydrogen applications in terms of gravimetric and volumetric density are 1.6 and 2.1 times higher (Table 1), respectively, than the values achieved to date using common 700-bar tanks. As far as we know, only the state-of-the-art 700-bar hydrogen tank designed by Toyota holds a hydrogen density of approximately 5.7 wt% H_2 [12], just satisfying the present target of DOE. Ammonia (NH_3) is also highly valued as a potential hydrogen storage option except compressed H_2 gas, owing to its high hydrogen density (17.8 wt% and 0.120 kg H_2 L^{-1} for gravimetric and volumetric H_2 density), low storage pressure and stability for long-term storage as well as high flexibility in its utilization [13]. In this regard, NH_3 can fulfill the demand to store the energy in time (stationary energy storage) and in space (energy export and import). However, NH_3 encounters high energy demand in both synthesis and decomposition for indirect utilization by the release of H_2. In case of liquid H_2, in spite of a much higher volumetric density (0.071 kg H_2 L^{-1}) that even surpasses the ultimate targets of DOE at the temperature as low as -253 °C, the inevitable hydrogen loss resulted from heat transfer and a large amount of energy consumed to liquefy hydrogen severely impede its practical applications [8, 14]. As same as liquid H_2, besides the much unavoidable energy consumption required in the high-pressurized compression, the high cost and latent safety risks of hydrogen refueling stations are the obstacles for the large-scale utilization in civilian vehicles. Admittedly, solid hydrogen storage materials [15] are the most acceptable hydrogen carriers and have received a great deal of attentions due to their ideal hydrogen density, reliable safety and numerous modification methods that have been developed to tailor their practical dehydrogenation capacities in recent years. Here, a comparison of some typical hydrogen mediums in terms of cost, hydrogen storage capacity and safety is summarized, as shown in Table 2.

Table 1 Current states vs targets for onboard H_2 storage for light-duty fuel cell vehicles [11]

Storage targets	Gravimetric kWh kg^{-1} (kg H_2/kg system)	Volumetric kWh L^{-1} (kg H_2/L system)	Cost[1] $/kWh ($/kg H_2)
2020	1.5 (0.045)	1.0 (0.030)	$10 ($333)
2025	1.8 (0.055)	1.3 (0.040)	$9 ($300)
Ultimate	2.2 (0.065)	1.7 (0.050)	$8 ($266)
Current status[2]			
700 bar compressed (5.6 kg H_2, type IV, single tank)	1.4 (0.042)	0.8 (0.024)	$15 ($500)

[1]Projected at 500,000 units/year

[2]FCTO Data Record #15,013, 11/25/2015: https://www.hydrogen.energy.gov/pdfs/15013 onboard storage performance cost.pdf

© The authors
https://doi.org/10.1007/s40820-021-00657-9

Table 2 A comparison between some typical lightweight materials and hydrogen mediums [16, 17]

Parameters	Solid				Non-solid	
Category	Metal hydride	Complex hydride	Microporous adsorbents		Liquid hydrogen	ammonia
Compound	MgH_2	$NaBH_4$	Activated carbon	MOF	H_2	NH_3
Gravimetric capacity (wt%)	7.6	10.7	2.1–2.6	6.1	1.4	1.89
Volumetric capacity ($g\ L^{-1}$)	110	116	20	20	125	114
Cost	Low	High	Low	Low	Low	Low
Thermolytic kinetics	Slow	Slow	Fast	Fast	Fast	Slow
H_2 release temperature (°C)	Very high (> 300)	Very high (> 500)	Low (-196 ~ 25)	Cryogenic (-196)	-253	350–900
Abundant	High availability	Schlesinger or Bayer method	High availability	High availability	High availability	High availability
Safety	Benign	Benign	Benign	Benign	Benign	Toxic and corrosive

In the mid and late of 2000s, the heavy intermetallic binary compounds were initially emerged as hydrogen storage materials owing to their good cycling performance and rapid kinetics under moderate conditions. However, the AB_2 and AB_5 types ($ZrFe_2$, $LaNi_5$, etc.), representative members of heavy metal alloys family, merely enable ≤ 2 wt% of hydrogen sorption because of the heavyweight and hydrogen non-absorptive trait of B side elements [9, 18–19]. To meet the hydrogen storage targets given by DOE, scientists and researchers have been focusing toward novel lightweight hydrides [20–22]. Among these hydrogen materials, the most fascinating hydrides are magnesium-based materials (MgH_2 as the host material) [23–25] and B-N compounds (borohydrides or ammonia borane) [26]. The gravimetric hydrogen densities of 7.6 wt% for MgH_2 and 18.5 wt% for $LiBH_4$ even exceed the value for on-board applications set by DOE. Recently, Shui's group [27] synthesized a multilayered Ti_2CT_x (T is a functional group) stack by incomplete hydrofluoric acid (HF) etching, and the as-prepared Ti_2CT_x showed an unprecedented hydrogen uptake of 8.8 wt% H_2 at room temperature and 60 bar H_2, which is much higher than the ultimate targets of DOE. Unfortunately, most of light metal-based materials are considered to be irreversible under mild conditions, so a serious of tailoring strategies have been developed for hydrolysis and thermolysis. For example, it was found that $ZrCl_4$ is an effective catalyst to considerably reduce the dehydrogenation temperature and activation energy for $LiBH_4$ [28]. Furthermore, the hydrogen produced by the thermal decomposition is always accompanied with the emission of other explosive or toxic gas such as CO and/or B_2H_6 [29]. Generally, PEMFCs are very sensitive to the impurity of hydrogen, and even a little amount of impurity may cause the poisoning the catalysts [30]. Compared with the above approach, pure hydrogen supply from hydrolysis of light metal-based materials, including metal hydrides and borohydrides via reacting with water without external heat input, has a number of advantages, such as suitable operation temperature and well-controlled hydrogen release. Especially, hydrogen supply via hydrolysis is a self-humidification process, and such humid hydrogen can be conveyed directly into PEMFCs without dehumidification treatment and any performance loss [31]. Different from liquid H_2 or gas-state hydrogen carriers that need further development and construction in infrastructures, such as the NH_3/H_2 pipelines, H_2/NH_3 refueling stations and liquefaction devices, the storage and transportation of metal hydrides and borohydrides hold low potential risk and low capital investment because they are largely compatible with the current transport infrastructure [13]. For Mg-based and Al-based materials, they can be stored and transported in the form of bulks. Moreover, the formation of a coherent passive layer deposited on the surface of bulks may prevent further oxidation of hydrolysable materials. With respect to borohydrides, $NaBH_4$, an example of the family of borohydrides, is a well-known hydrogen carrier due to its high hydrogen-storage capacity (10.8 wt%) [32, 33]. It is easily dissolved in alkaline aqueous solution for safe, stable and long periods of storage, leading to a highly convenient transportation. Therefore, the currently

available storage and transportation facilities and their regulation can be well utilized to increase the readiness for the adoption of light metal-based materials.

Hydrolysis enables hydrogen extraction from liquid water. However, the performance of hydrolysis reaction is subject to the operation temperature. The hydrogen generation rate will be significantly reduced in a low-temperature climate and the hydrolysis process could even be directly frozen in subzero circumstances. Methanol has a very low freezing point (-97 ℃); thus, hydrogen supply from methanolysis is considered optimal for real-time hydrogen production in low-temperature climate or subzero areas. At mild conditions, the reversible hydrogen storage systems like the metal-based hydrides have the advantages of fast hydrogen injection and durability for repeated recycling, whereas the hydrogen storage properties are plagued by the sluggish de-/hydrogenation kinetics, thermodynamic barriers (de-/rehydrogeneration temperature < 100 ℃, pressure < 10 atm) and cyclic performance [34]. In contrast, the device for hydrolysis hydrogen supply is very compact [35], and the hydrogen derived from water or light metal-based materials can be directly connected to the fuel cell to drive the motor. Significantly, water freight is safer and more convenient compared to high-pressure hydrogen storage and transportation. However, the controllability and utilization of enormous exothermicity of hydrolysis require further investigations.

In this review, we summarize the recent progress in the development of hydrolysis and alcoholysis of light metal-based materials, especially the Mg-/Al-based materials and borohydrides. To overcome the sluggish hydrolysis and low conversion, various methods have been developed, such as ball milling, catalysis, alloying, and solution modification. The different hydrolysis mechanisms of Al/Mg-based materials and sodium borohydride are discussed in detail. Furthermore, the recent advances in $NaBH_4$ regeneration process from hydrolysis by-product are discussed. $NaBH_4$ is considered as the most potential hydrolysable material.

2 Hydrogen Generation from Hydrolysis or Alcoholysis

The typical hydrolytic materials include metals/hydrides, ammonia borane (NH_3BH_3, denoted as AB) and borohydrides. Hydrogen supply from $NaBH_4$ hydrolysis was the most widely studied and has numerous advantages over the other hydrolytic materials, including half of hydrogen production from water, low operation temperature, environmentally benign by-product, well-controlled and high-purity hydrogen release [36–38], making it promising for on-board or onsite hydrogen supply. On the other hand, Mg- or Al-based materials are also widely discussed as hydrogen carriers, and they can supply high-purity H_2 according to real-time demands via contacting with water. Compared to costly borohydrides, hydrogen supply from the light-metal materials is affordable and sustainable because of the abundant content in the earth crust and the mature recycling process in the industry. The following sections mainly emphasize the hydrolysis/alcoholysis of borohydrides, Mg-/Al-based alloys and hydrides.

2.1 Highly Efficient Catalytic and Non-catalytic Alcoholysis/Hydrolysis of Borohydrides

Extensive efforts have been devoted to exploring highly efficient hydrolysis of borohydrides ($NaBH_4$, $Mg(BH_4)_2$, $LiBH_4$, etc.) or AB due to their excellent hydrogen storage capacities [39–41]. For hydrogen application in fuel cells, if the water produced in the fuel cell part is redirected to $LiBH_4$, then the H_2 generation capacity may increase to 37.0 wt% [42]. Compared with the expensive $LiBH_4$, $NaBH_4$ with a 21.1 wt% H_2 generation capacity (the water produced in the fuel cell part is recycled to react with $NaBH_4$ and it is not taken into account in the case) is preferred as a more superior hydrolysable material, but its hydrolysis suffers from sluggish kinetics in neutral aqueous solutions. To lower the high kinetic barrier to an extent that would give a hydrogen generation rate closing to the requirement of practical applications, a variety of non-noble metal catalysts have been developed, such as Fe, Co, Ni or Pt, Ru, and Pd [43–47]. Especially, in the hydrolysis of borohydride aided by M_3B (M = Cu, Ni, Fe), the catalytic activities are in the order of Cu < Ni < Co [48]. The Co-B-based types [49–52] are commonly admitted as reactive as noble metals and much more cost-effective, which exhibit saltant performance improvements. The enhanced performance results from the Co-B catalysts loaded on supports with a high surface distribution, where transition metals (Co, Ni, and Fe) act as active sites. The real hydrolysis by-product of $NaBH_4$ is $NaBO_2{\cdot}xH_2O$, and the real-time hydrolysis reaction is given as follows [53]:

© The authors https://doi.org/10.1007/s40820-021-00657-9

$$NaBH_4 + (2 + x)H_2O \rightarrow NaBO_2 \cdot xH_2O + 4H_2 \quad (1)$$

That is, $NaBH_4$ could produce four equivalents of hydrogen through the hydrolysis process. Recently, Appiah-Ntiamoah et al. [54] synthesized a novel catalyst with a core–shell structure, where Co was loaded upon Fe_3O_4@C "active" support. The unique properties of the "active" Fe_3O_4@C promoted a synergistic catalytic reaction involving Co, Fe_3O_4, and C during $NaBH_4$ hydrolysis as shown in Fig. 1, delivering a hydrogen generation rate up to 1746 mL (g min)$^{-1}$. Holbrook [55] believed that the hydrolysis mechanism with transition catalyst could be classified into five steps as shown in Fig. 1a. Firstly, the chemisorption of BH_4^- on the metal atom site produces M-BH_3 and M-H (step 1–3). Then, an electron from M-BH_3 is transferred to the M site and BH_3 is discarded, so the electronegative M site attracts H^+ in water to form a new M-H. And a consumption of the two M-H can release one H_2 molecule, then the BH_3 legacy and OH– will form $BH_3(OH)^-$ (step 4–5). Subsequently, the stable intermediate $BH_3(OH)^-$ successively provides three active hydrogens, which will attack three H_2O to form BOH_4^- finally and release 3 mol of H_2 (step 5–6). However, Fe exposed in the pores and Co could also from Fe_3O_4@C–Co to catalyze hydrogen release according to the mechanism proposed by Pena-Alonso via a synergistic effect as shown in Fig. 1b where hydrogen is firstly produced in the 3rd step, and the entire reaction path is shortened. Moreover, the reusability and stability of Fe_3O_4@C–Co composite were investigated via successive catalytic runs, and there was negligible loss in the amount of H_2 generated after 5 runs. The Fe_3O_4@C–Co composite showed high recyclability performance in catalytic activity and structural integrity, signifying its real-life application prospects. Furthermore, Patel's team [56] doped with various transition metals in Co-B-based binary catalysts and explored the hydrolysis properties as shown in Fig. 2. The Co–B-based ternary or quaternary catalysts may display better catalytic activity than binary catalysts. Table 3 summarizes recent advances on Co-based catalysts and their catalytic performances for $NaBH_4$ hydrolysis. More information and applications about hydrogen production from $NaBH_4$ for fuel-cell systems could be referred from a recent review [57].

AB is considered as a leading contender in promising chemical hydrogen-storage materials for various applications due to its high hydrogen density (19.6 wt%) and high stability both in solid state and solution under ambient conditions, as well nontoxicity and high solubility [33, 73]. It can release three equivalents of hydrogen vis thermolysis, but the third-step dehydrogenation requires more than 1200 ℃. Similarly, the developed catalysts for the hydrolysis of $NaBH_4$, such as noble metal-based NPs and Co-based NPs deposited on supports, can also impel AB hydrolysis as well. Li et al. [74] synthesized CVD-Ni/ZIF-8 by chemical vapor deposition, which could promote ammonia borane to release 3 equivalents of hydrogen in 13 min. Later, Wang et al. [75] deposited Ni NPs in ZIP-8 by $NaBH_4$ reduction method, which promoted AB to complete reaction in 0.3 M NaOH solution within 5 min with a TOF value of 85.7 mol_{H2} mol_{cat}^{-1} min^{-1}. Interestingly, it was found that H^+ in the acid could slow the reaction, and a certain concentration of OH^- remarkably improved hydrogen evolution. Therefore, a switch was designed to control hydrogen supply by adjusting the pH value of the solution. In addition, the reusability of the nanocatalyst NiNPs/ZiF-8 was examined by the continuous addition of a new proportion of AB aqueous solution when the previous run was completed. It was found that the activity of NiNPs/ZiF-8 was essentially retained until the fifth run and there was almost no loss in the amount of H_2 generated during the cycling test. He et al. [76] also got the same result that OH^- in aqueous solution is crucial in determining the hydrolysis kinetics of AB through the kinetic isotope effect (KIE). Wang et al. [77] further explored the hydrolysis mechanism of Ni_2Pt@ZIF-8 and found that OH^- acted as a catalyst promoter, making the NP more electron-rich, which could favor the oxidative addition of water, as shown in Fig. 3. The presence of OH^- boosts H_2 evolution that becomes 87 times faster than in its absence with Ni_2Pt@ZiF-8. The kinetic isotope effects using D_2O showed that cleavage by oxidative addition of an O–H bond of water onto the catalyst surface is the rate-determining step of this reaction, enabling significant progress in catalyst design toward convenient H_2 generation from hydrogen-rich substrates in the near future.

Although the introduction of the catalyst can enhance the reaction to some extent, the difficulty and cost in recovering the catalyst, however, is an issue. Therefore, it is required to develop catalyst-free hydrogen supply systems from light-metal-based materials. Recently, Ouyang and co-workers investigated the non-catalytic hydrolysis of some borohydrides [36, 78, 79]. For instance, they found that the hydrogen generation rate for $NaBH_4$ hydrolysis could be accelerated by doping with $ZnCl_2$ without involving catalysts. It was

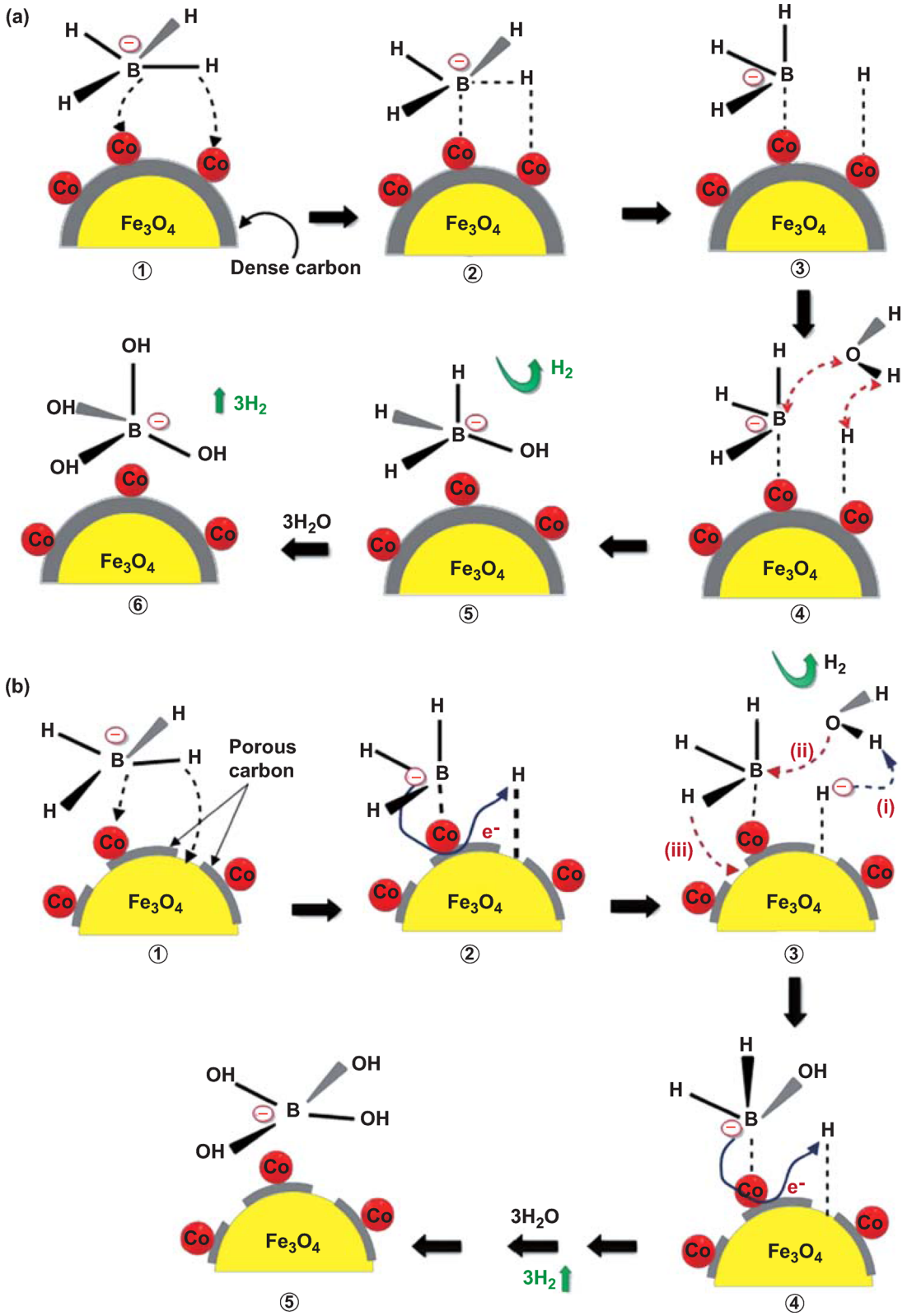

Fig. 1 Schematic illustration for $NaBH_4$ hydrolysis on **a** Fe_3O_4@C–Co and, **b** Fe_3O_4@C–X–Co (X = temperature). Reprinted with permission from Ref. [54]. Copyright 2019 Elsevier

© The authors
https://doi.org/10.1007/s40820-021-00657-9

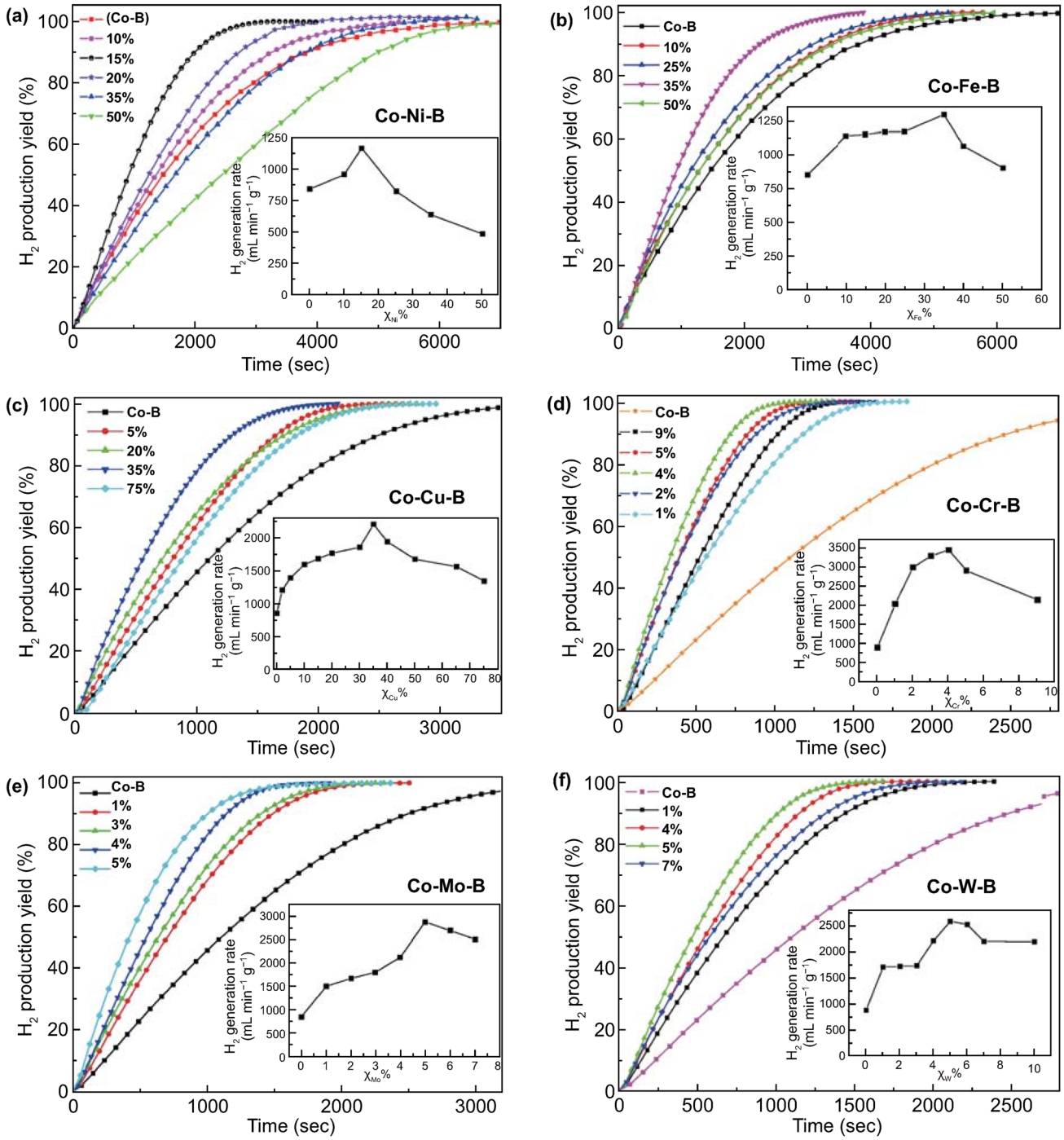

Fig. 2 Hydrogen generation yield as a function of reaction time obtained by hydrolysis of alkaline $NaBH_4$ (0.025 M) with **a** Co–Ni–B, **b** Co–Fe–B, **c** Co–Cu–B, **d** Co–Cr–B, **e** Co–Mo–B, and **f** Co–W–B with different χ_M values (where M = Ni, Fe, Cu, Cr, Mo, and W). Insets show the maximum H_2 generation rate (R_{max}) as a function of χ_M. Reprinted with permission from Ref. [56]. Copyright 2010 Elsevier

found that $NaBH_4$-35 wt% $ZnCl_2$ achieved the optimal hydrogen yield of 1964 mL g^{-1} H_2 with a considerable hydrogen production rate of 1124 mL g^{-1} within only 5 min [79]. Interestingly, they observed the existence of $NaZn(BH_4)_3$ (Fig. 4) after ball milling the mixture of $NaBH_4$-$ZnCl_2$ and further investigated the hydrolysis performance of pure

Table 3 Comparison of some Co-based catalysts and their catalytic performance for $NaBH_4$ hydrolysis

Catalyst	HGR (mL H_2 (g_{cat} min) $^{-1}$)	Preparation method	Activation energy (kJ mol^{-1})	Refs.
Fe_3O_4@C–Co	1746	Hydrothermal method–thermal treatment	47.3	[54]
Co–Fe_3O_4–CNT	1213	Stepwise precipitation–microwave-assisted reduction	42.8	[58]
PAN/$CoCl_2$–CNT nanofibers	1255	Electrospinning	52.9	[59]
Co/Fe_3O_4@C	1403	Wetness impregnation–chemical reduction	49.2	[44]
Co_3O_4 macrocubes	1498	Hydrothermal method	48.0	[60]
Co_3O_4 NA/Ti	1940	Hydrothermal treatment–annealing	59.8	[61]
Co–B/AT	1420	Impregnation–chemical reduction method	56.32	[49]
CoB/o–CNTs	3041	Wetness impregnation–chemical reduction	37.6	[50]
Co–La–Zr–B nanoparticle	102	Chemical reduction	51.00	[62]
p(AAm)–Co	1926	photopolymerization technique	39.7	[63]
$NiCo_2O_4$ hollow sphere	1000	Hydrothermal method	52.2	[64]
Carbon black supported Co–B	8034	Reduction–precipitation route	56.7	[65]
$LiCoO_2$/Ru	3000	Microwave-assisted polyol process	70.4	[45]
Co–Ni–B/Cu sheet	14,778	Electroless plating	42.8	[51]
Co–W–P/Cu sheet	5000	Electrodeposition	22.8	[66]
Ru–SZ	9100	Sol–gel method	76	[46]
Co–Ni–Mo–P/γ-Al_2O_3	10,125	Electroless deposition	52.4	[67]
Co–B/TiO_2	12,503	Chemical reduction	51.6	[52]
Co–P/Cu sheet	2275.1	Electroless plating	27.9	[68]
CoeP/Cu sheet	3300	Electroless plating	60.2	[69]
Co–P/Cu sheet	5956	Electroplating	23.9	[70]
Flower-like Co–P	1647.9	Electroless plating	47.0	[71]
Co–Mo–Pd–B	6023	Chemical reduction	36.4	[72]

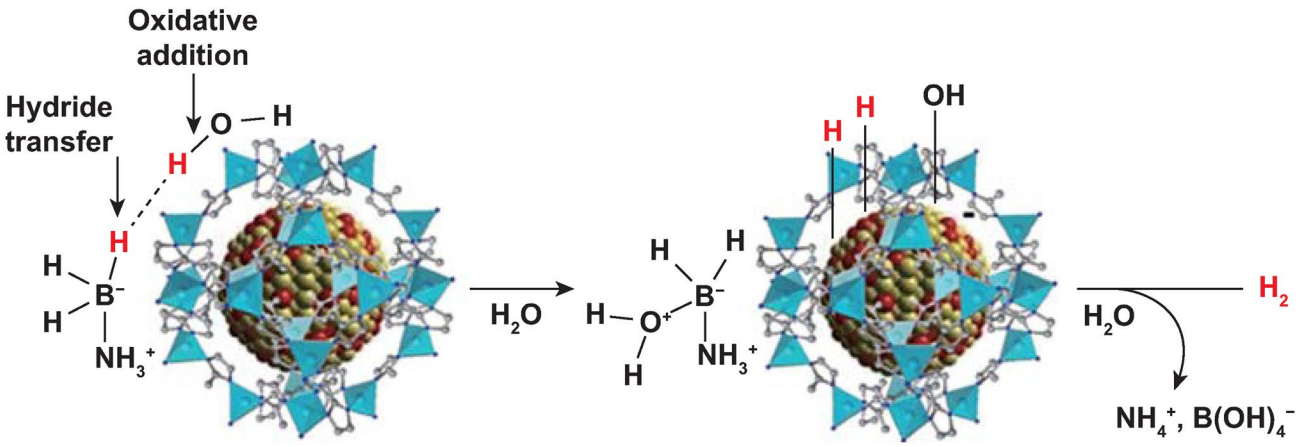

Fig. 3 Proposed mechanism for the hydrolysis of AB catalyzed by NiPt@ZIF-8. Reprinted with permission from Ref. [77]. Copyright 2018 American Chemical Society

$NaZn(BH_4)_3$ [36]. The results showed that $NaZn(BH_4)_3$ enabled the hydrogen release of 1740 mL g^{-1} in 5 min with a total hydrogen yield up to 97%. Because the ligands neighboring the metal cations in the borohydride involve the hydrogen elimination barrier and the stability of BH_4^- [80], they introduced NH_3 to achieve a rate-controlled hydrogen supply of $NaZn(BH_4)_3$ by forming its ammoniate. Similarly, they also studied the effect of ammonia complex number

© The authors https://doi.org/10.1007/s40820-021-00657-9

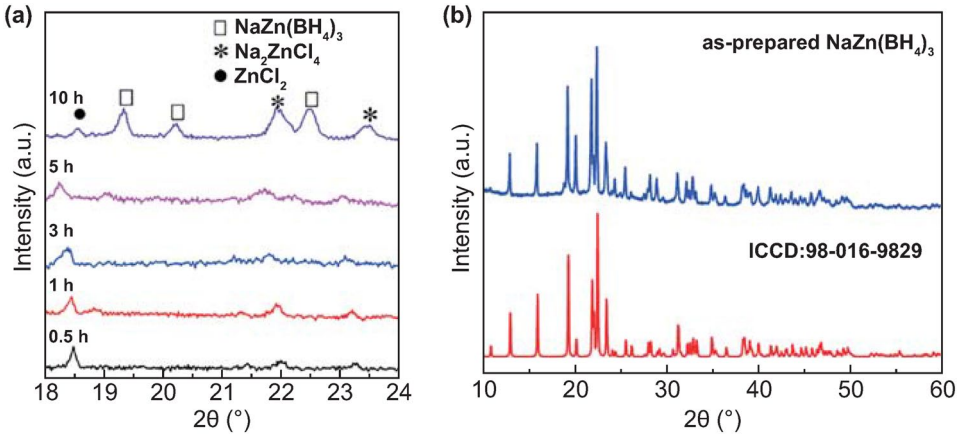

Fig. 4 XRD patterns of **a** $NaBH_4$-$ZnCl_2$ composites ball-milled for different durations. Reprinted with permission from Ref. [79], Copyright 2017 Elsevier, and **b** purified $NaZn(BH_4)_3$ and its standard PDF card. Reprinted with permission from Ref. [36], Copyright 2017 Royal Society of Chemistry

on hydrogen production kinetics by $Mg(BH_4)_2$ hydrolysis [78]. Obviously, the hydrogen evolution behaviors could be well-controlled via altering ammonia complex number upon $Mg(BH_4)_2$, whereas it sacrificed hydrogen yield. The hydrogen yields of $Mg(BH_4)_2{\cdot}0.5NH_3$, $Mg(BH_4)_2{\cdot}NH_3$, $Mg(BH_4)_2{\cdot}2NH_3$, $Mg(BH_4)_2{\cdot}3NH_3$, and $Mg(BH_4)_2{\cdot}6NH_3$ are 2376, 2029, 1780, 1665, and 1180 mL (H_2) g^{-1}, respectively. Similarly, $Mg(BH_4)_2$ can possess different hydrolytic behaviors when coordinated with various organic ligands (including $Mg(BH_4)_2 \times xE_2O$, $Mg(BH_4)_2 \times$ diglyme and $MgBH_4 \times 3THF$), with the larger the ligand and the higher the denticity, and the smaller amount of B_2H_6 being produced [81].

As is well known, the hydrogen generation performance would deteriorate markedly followed by temperature decrease. To solve this issue, alcoholysis and alcoholysis/hydrolysis composite hydrogen generation systems for $NaBH_4$ have been developed [37, 82–85]. For example, hydrogen release from $NaBH_4$ in ethylene glycol/water solutions in the presence of $CoCl_2$ catalyst could be quickly launched even at -10 ~ 20 °C, fulfilling 100% of fuel conversion within only a few minutes. What's more, the hydrogen density of the alcoholysis/hydrolysis composite system with optimized composition may reach 4 wt%. This demonstrated that a superior-performance hydrogen generation system with a wide range of operational temperature may be developed for practical hydrogen source for mobile/portable applications [37].

For $LiBH_4$ hydrolysis, the catalyst-free hydrolysis reaction never surpasses 50% of its theoretical yield due to the low solubility of the $LiBO_2$-based by-product in water that deposits on $LiBH_4$ and limits the full utilization of the hydride [86]. Kojima et al. [87] reported that the hydrogen densities increased with the increase in the dropped water ($H_2O/LiBH_4$) and followed by a reduction. These densities may show maximum values at $H_2O/LiBH_4 = 1.3$. To enhance the sluggish kinetics and low conversion efficiency for $LiBH_4$ hydrolysis, a series of strategies have been adopted toward H_2 release at approximately a stoichiometric equivalent, including the hydrolysis system of $LiBH_4$ doped with multiwalled carbon nanotubes (MWCNTs) [88] or diethyl ether addition [89], the non-catalytic hydrolysis of $LiBH_4/NH_3BH_3$ composite system [90], and the catalytic hydrolysis reaction system of $LiBH_4$ solution over nano-sized platinum dispersed on $LiCoO_2$ (Pt–$LiCoO_2$) [91], etc. Considering the affordability and sustainability, it is imperative to develop low-cost and non-noble metal catalysts that hold similar activity and stability with noble metals in the conversion and utilization of $LiBH_4$ hydrolysis system. Recently, Zhu's group [92] firstly adopted the transition-metal chlorides ($CoCl_2$, $NiCl_2$, $FeCl_3$) to promote the hydrolysis behaviors of $LiBH_4$. Among the above catalysts, $CoCl_2$ showed faster hydrogen kinetics, delivering a hydrogen generation rate ranging from 421 to 41,701 mL H_2 min^{-1} g^{-1} with a maximum conversion of 95.3%. These values are much higher than the value of 225 mL H_2 min^{-1} g^{-1} with Pt-$LiCoO_2$. Moreover, NH_3 was introduced to tailor the uncontrollable kinetics of $LiBH_4$ by forming its ammoniates ($LiBH_4{\cdot}xNH_3$, x = 1, 2, 3). In the presence of $CoCl_2$, $LiBH_4{\cdot}xNH_3$ could stably release over 4300 mL H_2 g_{LiBH4}^{-1}

with a hydrogen capacity of ~ 7.1 wt% and a H_2 yield of 97.0%, while it reacts with a stoichiometric amount of H_2O. However, the difficulty in regenerating the utilized $LiBH_4$ and the associated high cost hamper their large-scale applications. In the near future, developing convenient and economical methods for $LiBH_4$ regeneration is a linchpin, as it acts as hydrogen carrier in off-/on-board applications.

2.2 Hydrogen Production via Hydrolysis of Mg-based Alloys or Its Hydrides

Compared to borohydrides, the hydrolysis from light metals and metal hydrides for down-to-earth hydrogen supply has a number of advantages, including low-cost, abundant element contents, environmentally benign products of oxidation, etc. [38, 93–95]. Generally, it is widely accepted that the hydrolysis reaction of Mg or MgH_2 is rapidly interrupted by a passive $Mg(OH)_2$ layer deposited on the surface of Mg-based materials, leading to poor hydrolysis performance. To date, numerous methods, such as ball milling, alloying, aqueous solution modification or catalysis [96–99], have been applied to enhance the sluggish kinetics. Recently, Ouyang' group [100] synthesized flower-like MoS_2 spheres via a one-step hydrothermal method. The as-prepared MoS_2 composes of many uniform spherical nanoparticles (Fig. 5), resulting in larger surface areas than its bulk counterpart. The Mg-10 wt% MoS_2 composite could release over 90% of theoretical hydrogen capacity in 1 min. Also, they investigated the catalytic effects of the transition metal Mo and its compounds (MoS_2, MoO_2, and MoO_3) upon hydrolysis of Mg in seawater [99]. The results showed that the distribution of MoS_2 catalyst in the Mg matrix became increasingly homogeneous with the increase in milling time (Fig. 6). The unique structure and uniformly dispersed MoS_2 could significantly accelerate the hydrolysis process of Mg. Moreover, the reusability and stability of MoS_2 were investigated via successive catalytic runs. As shown in Fig. 7, there was a slight drop in the amount of H_2 generated after 5 runs, and the catalytic activity of retrieved MoS_2 was completely retained without decrease in H_2 evolution rate. They believed that the markedly enhanced activity could be attributed to the synergistic effect of grinding and the galvanic corrosion between Mg- and Mo-based additives.

In addition to doping catalysts, alloying and ball milling have been proved to be effective means to enhance the hydrolysis performance of Mg. Ouyang et al. [97, 102–106] systematically studied the hydrolysis behaviors of Mg-RE alloy and its hydrides. They found that rare-earth elements could facilitate the hydrogen absorption of Mg-based alloys, resulting in higher hydrogen yields for the hydrolysis of hydrogenated Mg-RE. Ma et al. [107] revealed that Ni could promote the hydrogenation of $CaMg_{1.9}Ni_{0.1}$ under room temperature, as opposed to 450 °C for pure $CaMg_2$. Thus, the H-$CaMg_{1.9}Ni_{0.1}$ could achieve a hydrogen yield of 1053 mL g^{-1} in only 12 min,

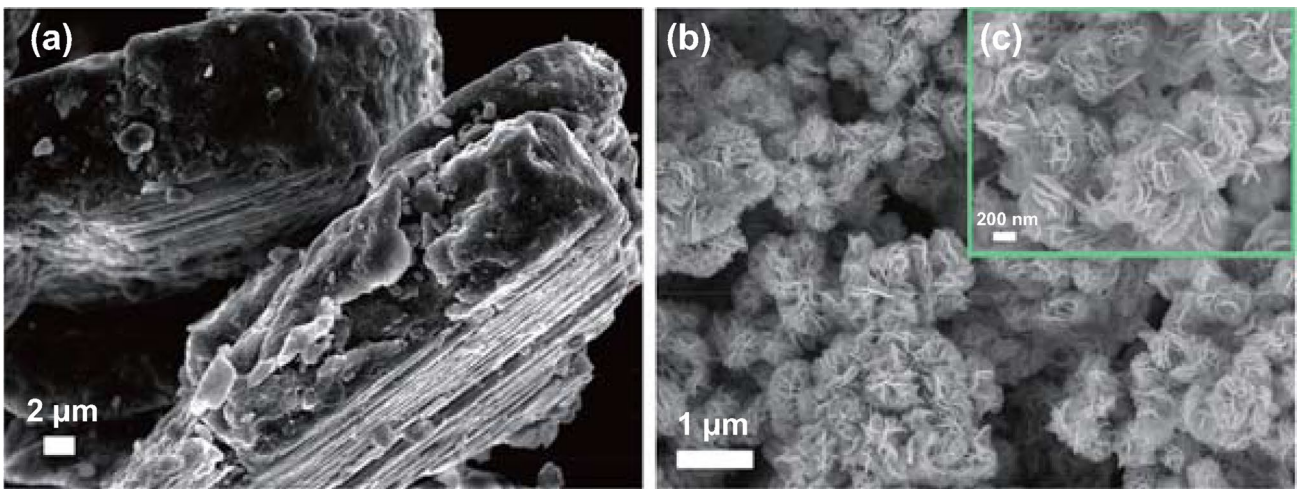

Fig. 5 SEM images of **a** bulk and **b** as-prepared MoS_2, **c** high-magnification SEM image showing a small zone of the as-prepared MoS_2. Reprinted with permission from Ref. [100]. Copyright 2017 Elsevier

© The authors https://doi.org/10.1007/s40820-021-00657-9

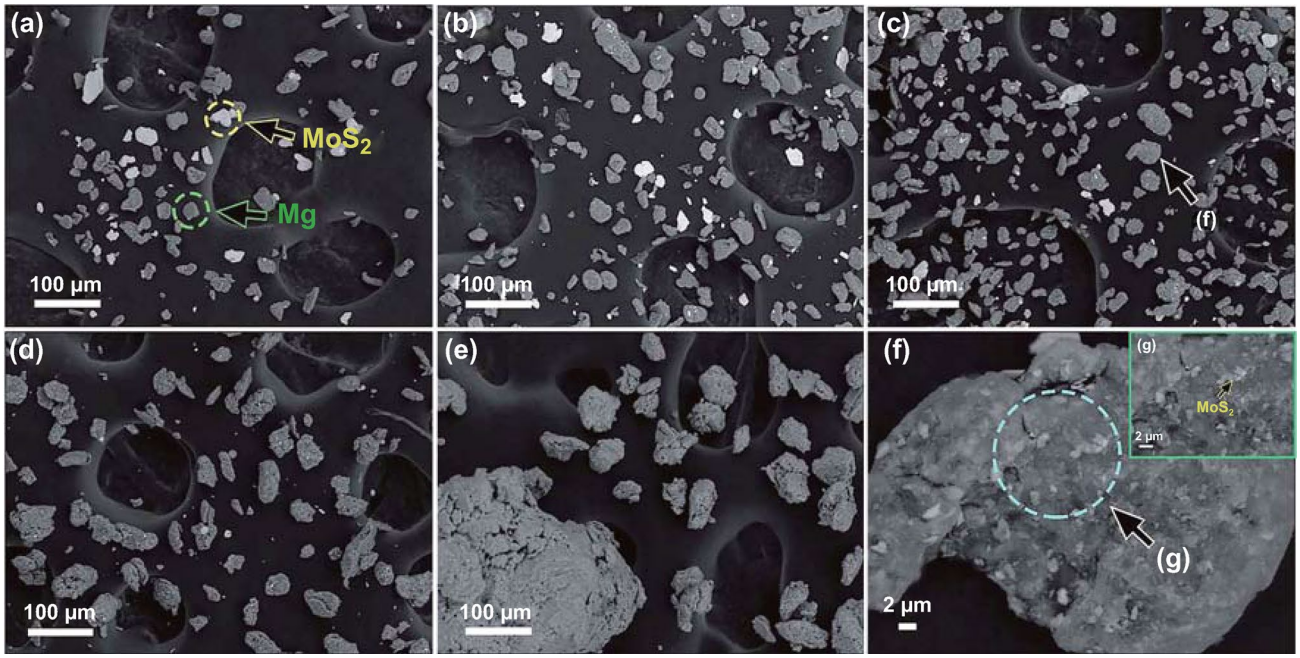

Fig. 6 SEM images of the Mg-10 wt% MoS_2 composite milled for various durations: **a** 0.1 h, **b** 0.5 h, **c** 1 h, **d** 3 h, and **e** 5 h, **f** and **g** high-magnification SEM images showing a small zone of the Mg-10 wt% MoS_2 composite milled for 1 h. Reprinted with permission from Ref. [99]. Copyright 2017 Royal Society of Chemistry

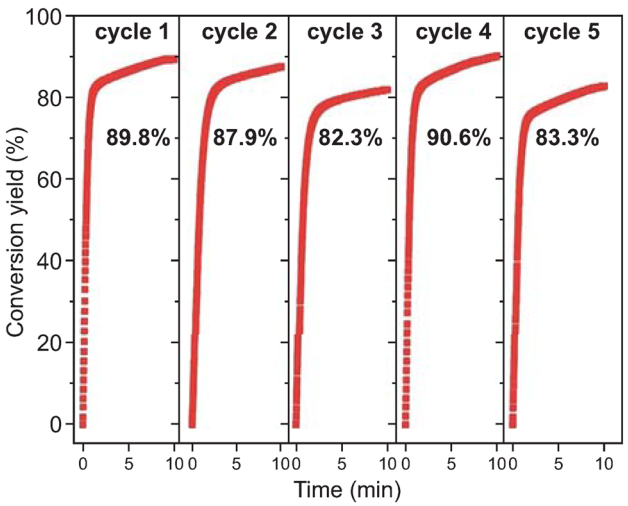

Fig. 7 Cyclic curve of hydrogen evolution via hydrolysis of Mg-10 wt% retrieved MoS_2 milled for 1 h in seawater. Reprinted with permission from Ref. [99]. Copyright 2017 Royal Society of Chemistry

approximately twice as much as that of $CaMg_{1.9}Ni_{0.1}$. In this regard, they doped a small amount of Ni toward $CaMg_2$ via ball milling [108]. The hydrogen yield of the hydrogenated $CaMg_2$-0.1Ni sample could increase from 853 to 1147 mL H_2 g^{-1} in 5 min with hydrogenation durations ranging from 0.5 to 1.5 h. On the other hand, Ouyang et al. [109] found that the hydrolysis properties of Mg can be greatly enhanced with the addition of expanded graphite by plasma-assisted milling. The obtained Mg-graphite composite could release 614.3 mL H_2 g^{-1} in 25 min with a hydrolysis conversion rate of 83.5%. They also synthesized refined hydrogenated MgLi (H-MgLi) by reactive ball milling [110], producing ~ 15.8 wt% hydrogen in 5 min. As same as $NaBH_4$, the hydrogen generation behaviors of Mg would deteriorate markedly followed by decreased temperature. To remove the troublesome freezing issue of the water solution system in low-temperature conditions, Ouyang et al. [111] adopted pure methanol, methanol/water and methanol/ethanol solutions to react with $CaMg_2$ alloy and its hydrides for hydrogen generation. The as-prepared $CaMg_2$ could generate 858 mL H_2 g^{-1} within only 3 min at room temperature, while it reacted vigorously with methanol, as opposed to a low hydrogen yield with ethanol and water (395 and 224 mL H_2 g^{-1} within 180 min, respectively). Even at – 20 °C, there was still over 600 mL H_2 g^{-1} released at a conversion rate of 70.7% within 100 min for methanolysis, demonstrating its

prominent advantage for hydrogen production, especially in winter or subzero areas.

Aqueous solution modification is also an effective strategy to tailor the hydrogen behaviors of Mg-based materials. In real application, large excess of water is required to ensure complete hydrolysis of Mg, resulting in significant capacity loss. The formation of insoluble $Mg(OH)_2$ enables simple separation and repeated using of water, which minimizes the hydrogen capacity loss caused by the excessive water. In this regard, Li et al. [112] solved the issue by using MgH_2 nanoparticles together with the promotion effect of $MgCl_2$ solution. A near-theoretical amount of H_2 (1820 mL g^{-1}) was released within 20 min in 1 M $MgCl_2$ solution without any pretreatment of the MgH_2 nanoparticles (800 nm). By separating $Mg(OH)_2$ through filtration and recycling the $MgCl_2$ solution, the hydrogen capacity of this system may approach the theoretical value of 6.45 wt% with continuous MgH_2 and water feeding. Recently, Tan et al. [113] reported that the hydrolysis performance of Mg_2Si could be notably improved by using NH_4F solution. The fluorine ion was introduced to restrain the release of silanes during the hydrolysis reaction of Mg_2Si. Due to its high chemical affinity to silicon ion, it is possible for F^- to break the Si–H bond and form H_2 and SiF_6^{2-} in aqueous solution. As the concentration of the NH_4F solution increased to 13.0%, the hydrogen yield of Mg_2Si reached the maximum, producing 616 mL H_2 g^{-1} in 30 min at 25 °C. The L.G. Sevastyanova et al. [101] systematically explored the effect of salt solutions and the transition metals on magnesium hydrolysis (Fig. 8) and found (1) the NH_4Cl solution exhibited the fastest initial reaction rate, but the conversion yield reached the maximum in NaCl solution, (2) aqueous solutions of alkaline or alkali earth metal chlorides at a salt content over 3 wt% would effectively improve the hydrolysis performance (the optimal amount being 4–15 wt%), (3) the transition metals can also cause reduction of the hydrogen yield if it is over 10 wt%. Correspondingly, Table 4 lists the varieties of some Mg-based materials and their hydrolysis properties. Nearly all hydrolysis materials enable the solution concentration being at least 3 wt% and the amount of oxidation addition not exceeding 10 wt%.

2.3 Hydrogen Production via Hydrolysis of Al-based Alloys or Its Hydrides

The distribution of aluminum is more abundant than magnesium, being third only to oxygen and silicon. Aluminum is a safe and cheap metal as well as electrochemically active element; thus, it may be a more appropriate candidate for the process of hydrogen production [31, 128]. The catholic use of aluminum is for the applications in batteries [129], like the aluminum–air battery that has an aluminum-based anode. While this aluminum-based battery has potential prospect in electric

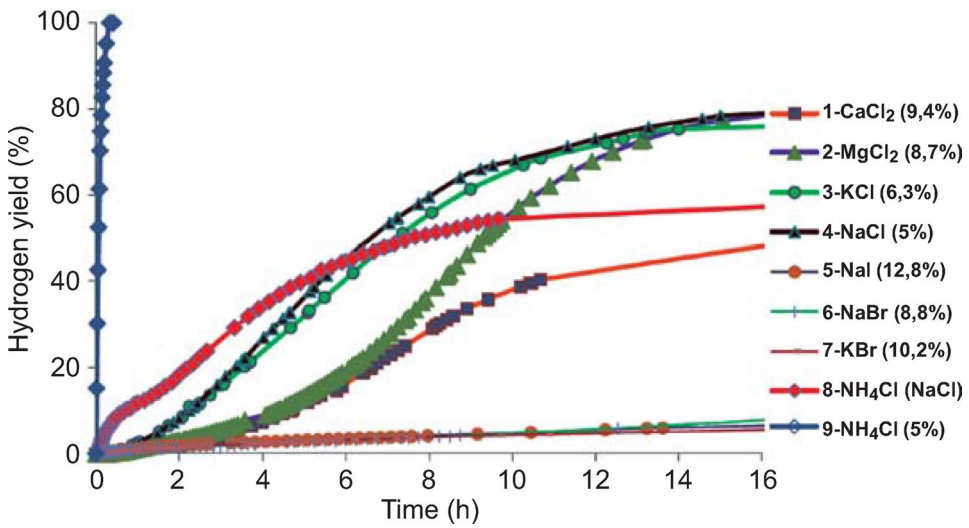

Fig. 8 Yields of hydrogen release due to magnesium powder oxidation in the presence of alkali, alkaline earth and ammonia halides (1 g of Mg in 30 mL of salt solution). Halide concentration was maintained approximately the same: 0.85 M (curves 1–7); 0.93 M for NH_4Cl (curve 9) and 0.31 M NH_4Cl + 0.85 M NaCl (curve 8). Reprinted with permission from Ref. [101]. Copyright 2014 Elsevier

© The authors
https://doi.org/10.1007/s40820-021-00657-9

Table 4 Comparisons of some ball-milling Mg-based materials and their hydrolysis performances

Materials	Solution	Hydrogen yield (%)	HGR (mL H_2/(g min)$^{-1}$)	Activation energy (kJ mol^{-1})	Refs.
Mg–10 wt% MoS_2	3.5% NaCl solution	90.4% in 1 min	–	12.9	[100]
Mg–10 wt% MoO_3	3.5% NaCl solution	91.7% in 10 min	2423	12.1	[99]
Mg–10 wt% MoO_2	3.5% NaCl solution	88.0% in 10 min	1933	14.3	[99]
Mg–10 wt% Mo	3.5% NaCl solution	86.5% in 10 min	751	27.6	[99]
Mg–10 wt% $CoCl_2$	Pure water	93.4% in 30 min	524	–	[114]
Mg–10 wt% $FeCl_3$	Pure water	98% in 2 min	1479.7	–	[115]
H–Mg_3La	Water	88% in 20 min	43.8	–	[105]
H–$Mg_{17}La_2$	Water	60.1% in 21 min	40.1	–	[105]
H–$Mg_3CeNi_{0.1}$	Pure water	57.4% in 10 min	276	–	[97]
H–$CaMg_{1.9}Ni_{0.1}$	Pure water	94.6% in 12 min	–	32.9	[107]
H–MgLi	Pure water	82% in 5 min	–	10.6	[110]
H–MgLi	1 M $MgCl_2$ solution	90% in 30 min	–	24.6	[110]
Mg–10% In	Seawater at 30 °C	93% in 10 min	444	12.4	[116]
Mg–10% In	Methanol at 20 °C	95% in 1 min	6900	–	[116]
Mg–Mg_2Cu eutectic alloy	3.5% NaCl solution	90% in 20 min	–	36.91	[117]
Mg–Mg_2Sn eutectic alloy	3.5% NaCl solution	90% in 20 min	–	38.19	[117]
Mg–90wt% $NdNiMg_{15}$	3.5% NaCl solution	100% in 15 min	60	–	[118]
Mg–Mg_2Si	0.5 M $MgCl_2$ solution	90% in 60 min	–	9.5	[93]
Mg–5 wt% G–5 wt% Ni	3.5% NaCl solution	95% in 2 min	–	14.34	[119]
Mg–10wt%Nd_2O_5	3.5% NaCl solution	100% in 30 min	–	31.46	[119]
30 wt% Ca-Mg hydrides	Deionized water	69.9% in 5 min	–	8.3	[120]
Mg-3% mol Al	Water	93.86% in 60 min	455.9	–	[121]
$4MgH_2$-$LiNH_2$	Water	72.7% in 50 min	887.2	–	[38]
MgH_2	4.5 wt% NH_4Cl solution	81% in 30 min	–	30.373	[98]
$(Mg10Ni)_{95}Ce_5$	Seawater	87% in 15 min	149.4	33.8	[122]
$(Mg10Ni)_{95}Ce_5$-EG-MoS_2 composite	Seawater	95% in 1 min	773	14.5	[122]
$(Mg–10Ni)_{85}La_{15}$	Distilled water	12.8% in 135 min	0.4683	–	[123]
$(Mg10Ni)_{95}Ce_5$	3.5 wt% NaCl solution	92% in 200 min	–	27.11	[124]
Mg10Ni–5wt%EG–5wt%MoS_2	3.5 wt% NaCl solution	91% in 5 min	148.16	9.26	[125]
Mg–25wt%Ni	3.5 wt% NaCl solution(48 °C)	60.3% in 30 min	48.28	9.57	[126]
Mg–30wt%Ce	3.5 wt% NaCl solution(48 °C)	85% in 30 min	171.88	14.65	[126]
Mg–30wt%La	3.5 wt% NaCl solution(48 °C)	90.2% in 30 min	74.52	23.88	[126]
$Mg_{10}Ni$–5 wt% MoS_2	3.5 wt% NaCl solution	67% in 15 min	1480	18.79	[127]

vehicles, it is inhibited by the undesirable parasitic corrosion reaction or the formation of a dense oxide layer. But the reaction actually produces hydrogen.

In addition, OH^- can dissolve the passive layer and form AlO_2^- to generate hydrogen even at room temperature. Taking the most commonly used NaOH solution as an example, the hydrogen generation is proposed as follows [130]:

$$2Al + 6H_2O + 2NaOH \rightarrow 2NaAl(OH)_4 + 3H_2 \quad (2)$$

$$NaAl(OH)_4 \rightarrow NaOH + Al(OH)_3 \quad (3)$$

$$2Al + 6H_2O \rightarrow 2Al(OH)_3 + 2H_2 \quad (4)$$

$$2Al + 4H_2O \rightarrow 2AlOOH + 3H_2 \quad (5)$$

Initially, the hydrogen generation reaction consumes sodium hydroxide, but when the $NaAl(OH)_4$ concentration exceeds the saturation limit, it leads to the NaOH regeneration process accompanying aluminum hydroxide formation. Therefore, only water is consumed during the whole hydrogen supply as shown by the reactions (4 and

5), and the hydrolysis by-products are the non-polluting bayerite ($Al(OH)_3$) and boehmite (AlOOH) [2, 131, 132]. Though the addition of OH^- is considered as the simplest and the most effective approach for promoting the Al/H_2O reaction [133], the use of an aqueous NaOH solution causes corrosion of system apparatus. Therefore, novel technologies that enable a combination of a minimized quantity of NaOH and rapid H_2 generation kinetics are highly desirable. Wang et al. [134, 135] found that a combined usage of sodium hydroxide (NaOH) and sodium stannate (Na_2SnO_3) can simultaneously address the Al/H_2O reaction kinetics and alkali corrosion problems. The addition of a small amount of Na_2SnO_3 causes a remarkable decrease of NaOH concentration without compromising the hydrogen generation performance of the system. In comparison with the traditional Al/H_2O system using aqueous NaOH solution, the new system exhibits a series of advantages in hydrogen generation performance, manipulability and adaptability; all are relevant to the development of practical aluminum-based hydrogen generation systems for mobile or portable applications. Notably, aluminum can be regenerated from the by-products by mature industrial technologies, the Bayer process [136] from bauxite ore (AlOOH) and the Hall–H′eroult process [137] from alumina.

Since Belitskus [130] first proposed the Al–water reaction to provide hydrogen in the 1970s, crucial efforts have been put into action to overcome the hydrolysis obstacle caused by the formation of the Al_2O_3 layer. Ball milling, as a frequently used method for increasing the hydrolysis performance of Mg-based materials, has proved to be effective for Al-based materials [138–142]. Yan et al. [140] milled an Al-10 mol% LiH-10 mol% KCl mixture for 10 h and obtained a hydrogen yield of 97.1% in 10 min at 60 ℃. The effects of metal chlorides to aluminum were similar to magnesium in hydrolysis. Firstly, chlorides can decrease the grain size during ball milling, and secondly, chlorides can also raise galvanic corrosion of magnesium or aluminum. Thirdly, Cl^- could damage the $Mg(OH)_2$ or $Al(OH)_3$ layer. Except mechanical activation by ball milling, torsional pressure and ultrasonic assistance, chemical activation of aluminum, such as by alloying, is also applicable. Originally, mercury was utilized for chemical activation of aluminum [143]. While mercury is a toxic substance and is not recommended for use in large scale, the new method of alloying to activate aluminum for aluminum–water reaction is sought after [144–147].

It has been confirmed that the hydrolysis properties have been enormously boosted up by alloying low melting point metals (LMPM) such as Ga, In, Sn and Zn with Al. Bulychev et al. [144] investigated the hydrolysis properties of aluminum alloy containing different accounts of LMPM. They found that the hydrogen supply virtually did not proceed without the presence of gallium, and the absence of indium in the alloy also led to a sharp decrease in the hydrolytic ability. But this alloy showed a terrible stability even stored under an inert atmosphere or in vacuum. They believed that this might be related to the presence of dispersed solid phases and a liquid phase (eutectic) distributed over the grain boundary space (Fig. 9). Parmuzinaa [145] held a point of view that the liquid eutectics based on gallium brought about eutectic penetration into aluminum grain boundaries, which destructed the inter-crystal contacts and resulted in the formation of aluminum monocrystal powders covered by eutectic thin film. Dong et al. [148] demonstrated that the presence of a liquid phase in the Al–Ga and Al–Ga–In–Sn alloys was decisive for the alloys to react with water and produce H_2 with an average yield of 83.8% in all 80 trials. The reaction temperature correlated well with the reported Al–Ga binary eutectic melting point of 26.6 ℃ and Ga–In–Sn ternary eutectic melting point of 10.7 ℃. When they changed the reaction temperature to make the alloys completely solid without liquid phase distribution, no hydrogen was produced. Interestingly, in many experiments, it was found that at 20–30 ℃, hydrogen generation from Al–Ga alloys stopped after only a certain extent [147, 149–153], but the reaction would resume if the system temperature was raised to resuscitate the liquid eutectic phase.

However, compared to the binary and ternary systems, the activity of the quaternary Al–Ga–In–Sn alloy was greatly improved and it could be fully reactive even at room temperature, indicating that the presence of a liquid eutectic phase in the Al-based alloy was essential. Liquid In_3Sn and $InSn_4$ were indeed observed in the Al–Ga–In–Sn quaternary system [154]. Qian Gao et al. [150] compared the hydrolysis properties of Al–Ga–$InSn_4$ and Al–Ga–In_3Sn alloys (Fig. 10). They concluded that the eutectic reaction of Al with $InSn_4$ was crucial, and Al could transfer from Al grains to intermetallic compounds to react with water continuously. Recently, Lu et al. [155] investigated the hydrolysis performance and activation mechanism of Al

© The authors https://doi.org/10.1007/s40820-021-00657-9

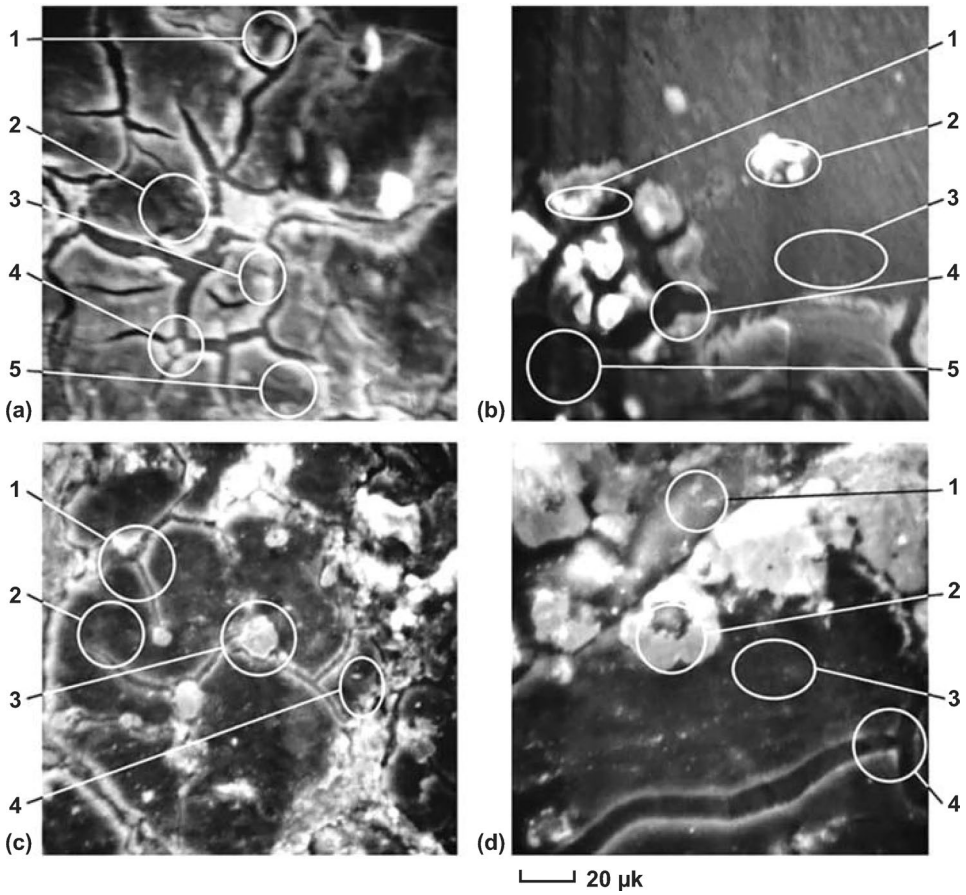

Fig. 9 SEM images of multicomponent aluminum alloy (Ga:In:Sn:Zn:Al = 5.3:2.0:5.4:7.3:80.0) sections (×800). **A** After preparation, **B** after annealing at 450 °C for 20 h. **C** and **D** after storing as-cast and annealed alloys for 1 month. Reprinted with permission from Ref. [144]. Copyright 2005 Elsevier

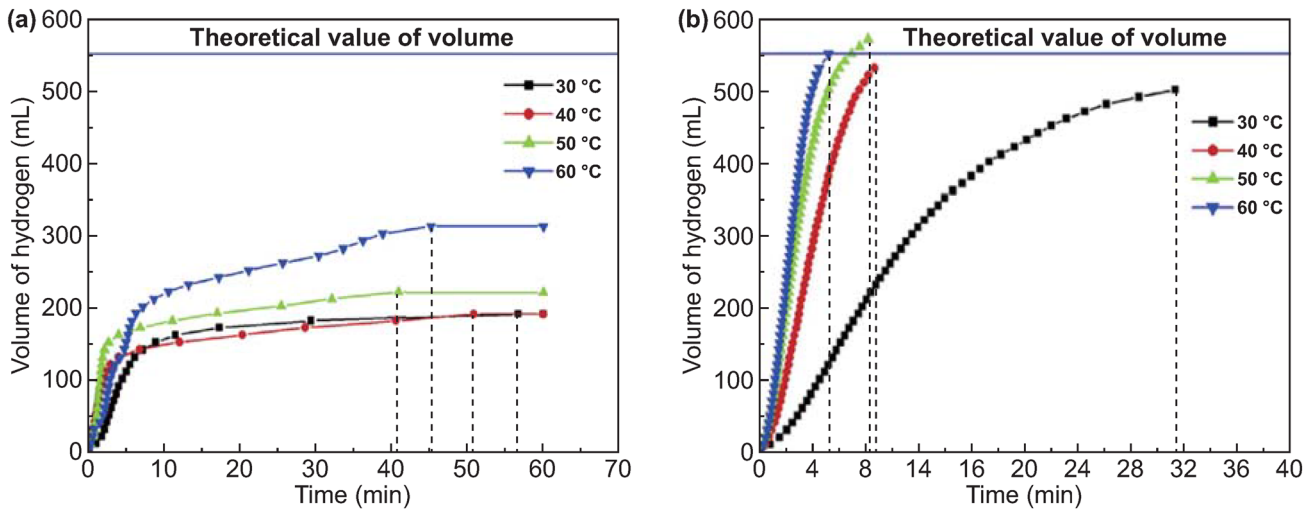

Fig. 10 Water temperature effect on hydrogen generation of Al–Ga–$InSn_4$ alloy and Al–Ga–In_3Sn alloy (0.5 g alloy ingot in 100 mL water), **a** Al–Ga–$InSn_4$ alloy and **b** Al–Ga–In_3Sn alloy. Reprinted with permission from Ref. [150]. Copyright 2015 Elsevier

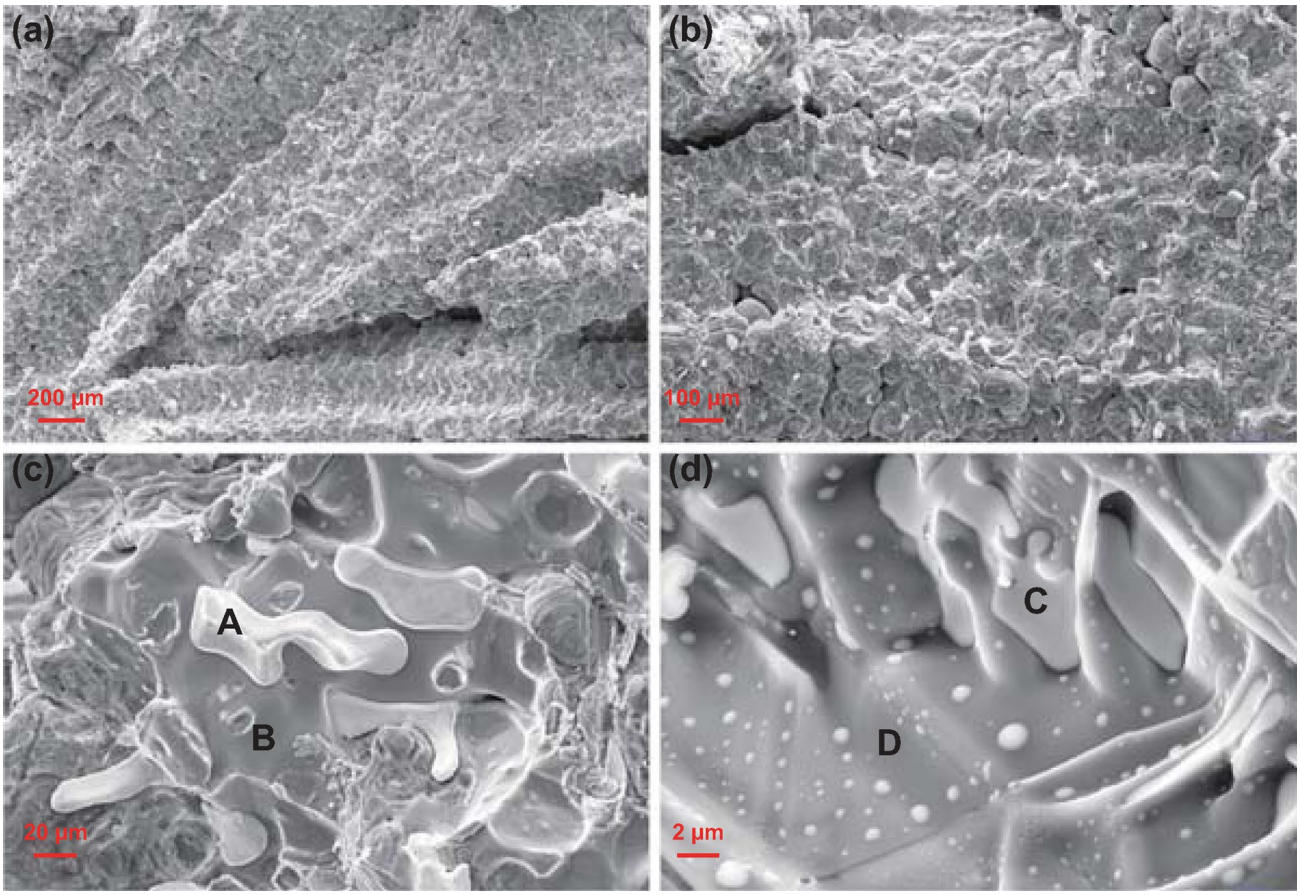

Fig. 11 SEM images of fracture surfaces of Al 85 wt%–$Ga_{68.5}In_{21.5}Sn_{10}$ alloy ingots, **a**, **b** images of the quaternary alloy, **c** enlarged image of intermetallic compounds, and **d** image of the LMPA at the grain boundary. Reprinted with permission from Ref. [155]. Copyright 2019 Elsevier

85wt%–$Ga_{68.5}In_{21.5}Sn_{10}$ alloy (Fig. 11). Combined with EDX analysis, the marked regions in the SEM images shown in Fig. 11c, d could be identified as In_3Sn phase (A), Al–Ga solid solution (matrix B), and C GaInSn liquid alloy (GIS) (C) and Al–Ga solid solution (matrix D). Especially, they emphasized the promotion of Al–water reaction with respect to the presence of low-melting eutectic liquid alloy GIS [156] and the In_3Sn phase. The Al–water reaction can be summarized in two steps. Firstly, a certain amount of Al atoms, which are solvated in the GIS and In_3Sn phases, are active and could react with the water freely. Secondly, the local temperature of the reaction site evidently increases due to a highly exothermic reaction, which can further promote the transportation of Al atoms to the interface and then react with water continuously.

It has been proven that alloying Al with low melting point metals is an effective approach to inhibit the formation of a coherent passivation layer and promote the hydrolysis kinetics. Liu et al. [153] tested Al on four different liquid alloys to produce hydrogen. It was found that aluminum completely dissolved in liquid $GaIn_{10}$ in 4 min, and the liquid metal surface remained shiny, meaning that $GaIn_{10}$ was stable during entire reaction process (Fig. 12). They designed pure Ga as a reactor and successively inlaid Al into it, and the process still achieved a great conversion yield after 5 times cycle without any dead-weight issues involved in system. Table 5 summarizes the varieties of some Al-based materials and their hydrolysis properties.

2.4 Hydrogen Production via Hydrolysis of Al-based Alloys or Its Hydrides

Hydrolysis of metals or metal hydrides is a highly exothermic reaction; full hydrolysis of 1 mol aluminum generates

© The authors https://doi.org/10.1007/s40820-021-00657-9

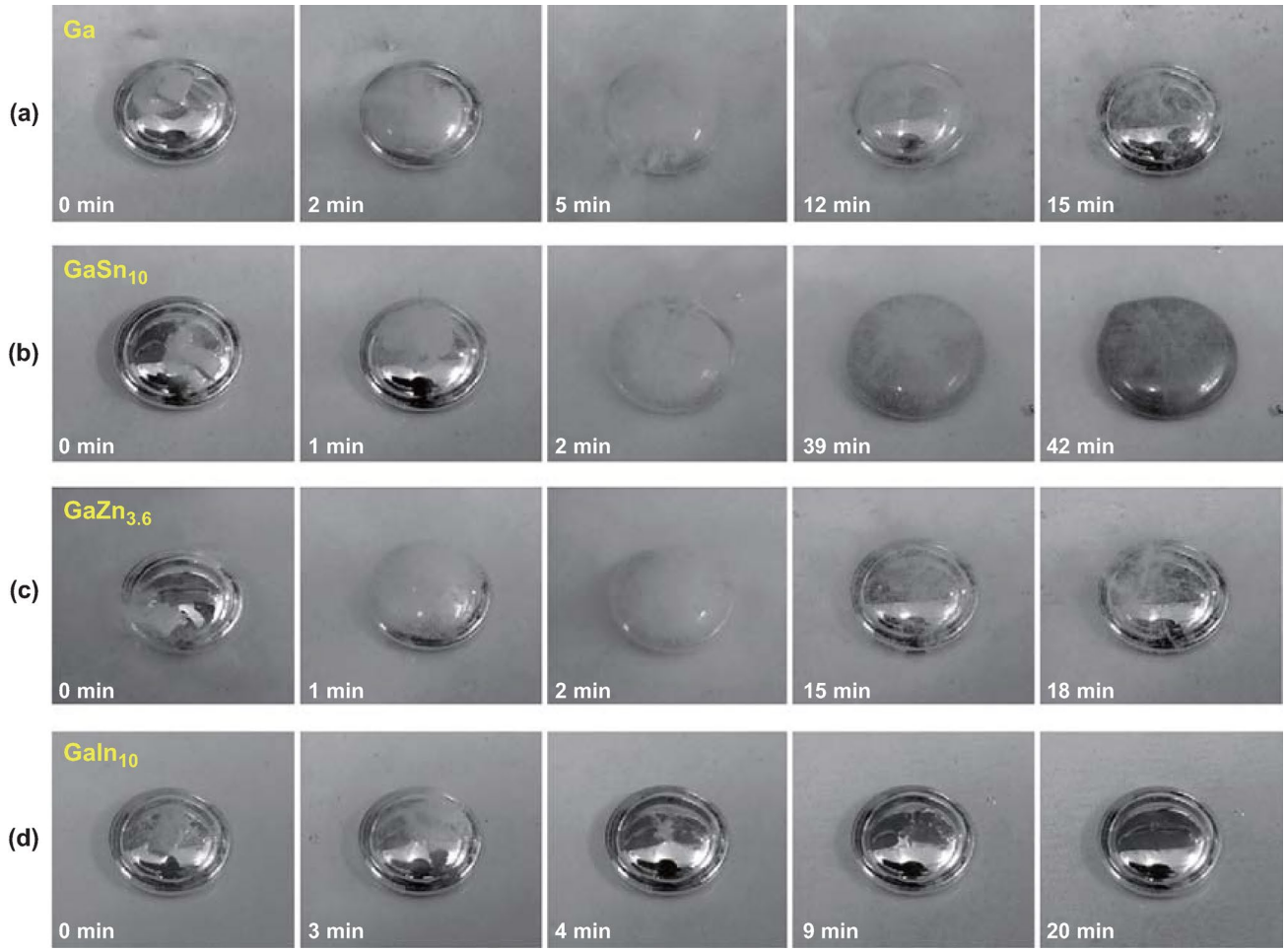

Fig. 12 Surface morphology comparisons among different liquid metals in aluminum–water reaction. **a** Ga. **b** $GaSn_{10}$. **c** $GaZn_{3.6}$. **d** $GaIn_{10}$. Reprinted with permission from Ref. [153]. Copyright 2016 Elsevier

437 kJ heat and 1.5 mol hydrogen. An amount of 363 kJ energy can be produced unambiguously from this 1.5 mol hydrogen if it can be thoroughly utilized. Similarly, the hydrolysis of 1 mol magnesium generates 354 kJ heat and 1 mol hydrogen. While the exothermicity is huge during the metal–water hydrolysis, there were only few efforts that tried to transform the thermal energy into other forms of useful energy. In particular, Zhong et al. [180] calculated the energy efficiencies in the hydrolysis cycles of MgH_2, H–Mg_3La and H–La_2Mg_{17}. The maximum energy efficiencies of MgH_2, H–Mg_3La, and H–La_2Mg_{17} were estimated to be 45.3%, 40.1%, and 41.1%, respectively, meaning roughly half of the energy released by the exothermic reaction was collected. Xiao et al. [181] firstly conceived and designed the Al-based hydrolysis battery, where the hydrolysis of Al was decoupled into a battery by pairing an Al foil with a hydrogen-storage electrode. In the hydrolysis battery, 8–15% of the hydrolysis heat was converted into usable electrical energy, leading to much higher energy efficiency compared to that of direct hydrolysis-H_2 fuel cell approach. The schematic illustration of the hydrolysis battery is shown in Fig. 13, where the hydrolysis reaction of Al is a redox reaction. Thus, Al foil and a Pd-capped YH_2 thin film were used as the anode and the cathode, respectively. As the hydrolysis battery was activated, the YH_2-Pd electrode would convert into YH_{2+x} phase ($x \approx 1$, the hydrogenated state), attaining the electrons flowed from Al. Desirably, the higher utilization of hydrolyzed thermal energy and more efficient kinetics controllability require further investigation.

Table 5 Comparisons of some Al-based materials and their hydrolysis performances

Materials	Solution	Hydrogen yield (%)	mHGR (mL H_2 (g min)$^{-1}$)	Activation energy (kJ mol^{-1})	Refs.
Al–15 wt% $Ga_{67}In_{20.5}Sn_{12.5}$	Tap water	87.79% in 2 h	–	–	[155]
Al–10 wt% $Ga_{68}In_{21}Sn_{0.75}Bi_{0.75}Zn_{0.75}$	Tap water	99.55% in 6 h	–	–	[155]
Al–10wt%Sn–5wt%Zn–5wt% MgH_2	Pure water	72.6%	159.6	17.57	[157]
Al–10 mol% LiH–10 mol% KCl	Water	97.1%	1221.1	–	[157]
Al/Ni/*n*NaCl (Ni/Al = 2:10, *n* = 24 wt%) mixtures	Distilled water	92.9%	3.1	54	[158]
Al–16 wt% Bi alloy	1 M NaCl solution	92.75%	92	–	[159]
Aluminum with zinc amalgam activation	Water	–	–	43.4	[143]
Al–5wt%In–3wt%Zn–2wt%NaCl mixture	Water	82.9%	250	–	[160]
Al–Ga–OMC nanocomposite	Pure water	100%	112	–	[161]
50 wt%Al–34 wt%Ga–11 wt%In–5 wt%Sn	Distilled water	~83.8%	78	43.8	[162]
Al–Ga–In–Sn alloy	Water	–	~700	53 ± 4	[149]
Al–Ga–In–Sn–Fe(92.5:3.8:1.5:0.7:1.5) alloy	Distilled water	100%	120	–	[152]
1 ml liquid Ga + 50 mg aluminum block	NaOH solution	~88.7	~37.5	–	[153]
Al–3wt%Ga–3wt%In		–	180	–	[154]
Al–3wt%Ga–3wt%In–5wt%Sn	Water	99%	1080	–	[154]
Al–12Bi–7Zn (wt.%) powder	NaCl solution	98%	–	–	[163]
Al alloy/NaCl/1 g-g-C_3N_4	Tap water	94%	280	21.28	[164]
Al–10 wt%Li–5 wt%Sn	Water	100%	44.3	–	[165]
incomplete core/shell structures Al–20wt%Bi	Distilled water	83%	–	–	[166]
Al–7.5%Bi–2.5%In composite	Pure water	95.5%	194	–	[167]
Al–Ga–In–Sn alloy	Water (50℃)	95%	–	–	[168]
Al–30 wt%Bi–10 wt%C composites synthesized by high-pressure torsion	Pure water(60℃)	100%	270	–	[169]
Al–15 wt%$NaMgH_3$-Bi-Li_3AlH_6	Distilled water	100%	1464	21.3	[170]
Al–10 wt%BiOCl–5 wt%LiH	Distilled water	94.9%	3178.5	26.9	[171]
(Al_2Ga)-8wt%In	Distilled water	70%	7.78	–	[172]
Al–1.0wt%Ga–1.5wt%In–3.0wt%$SnCl_2$-1.0wt%Bi_2O_3 composite	Tap water	92%	1030.5	20.08	[173]
Al–Ga–In_3Sn–Zn alloy	Deionized water	~95%	150	59	[174]
Al–Cu–Ga–In–Sn alloy	Distilled water	82.9%(50℃)	135	–	[175]
92Al–2 Mg–3.8 Ga–1.5In–0.7Sn	Distilled water	91%	14.8	–	[176, 177]
MHA–2%NaOH	0.5 M NaOH solution (55℃)	97.5%	421	29.3	[177]
Al with Graphite mixed $Al(OH)_3$ (G-2) catalyst	Distilled water	100%	68	27.94	[178]
Al/$Ni_{0.1}$/$Cu_{0.1}$/H_2O	Deionized water	70.6	96	–	[179]

3 Recent Advances in Regeneration Process of Borohydrides from Hydrolysis By-products

It has been demonstrated that hydrogen supply from $NaBH_4$ hydrolysis is a potential system for hydrogen generation. However, the hydrolysis reactions are plagued by irreversibility, and the resulting high-cost strikingly restrains the large-scale practical applications of these hydrolytic materials. Recently, Ouyang et al. developed a facile and economical method for $NaBH_4$ regeneration by recycling its real-time hydrolysis products ($NaBO_2{\cdot}2H_2O$ and $NaBO_2{\cdot}4H_2O$) for the first time without hydrides input [182, 183]. This may provide important insights for retrieving other hydrogen supply irreversible systems with high efficiency, such as $LiBH_4$ or $LiAlH_4$ production.

© The authors
https://doi.org/10.1007/s40820-021-00657-9

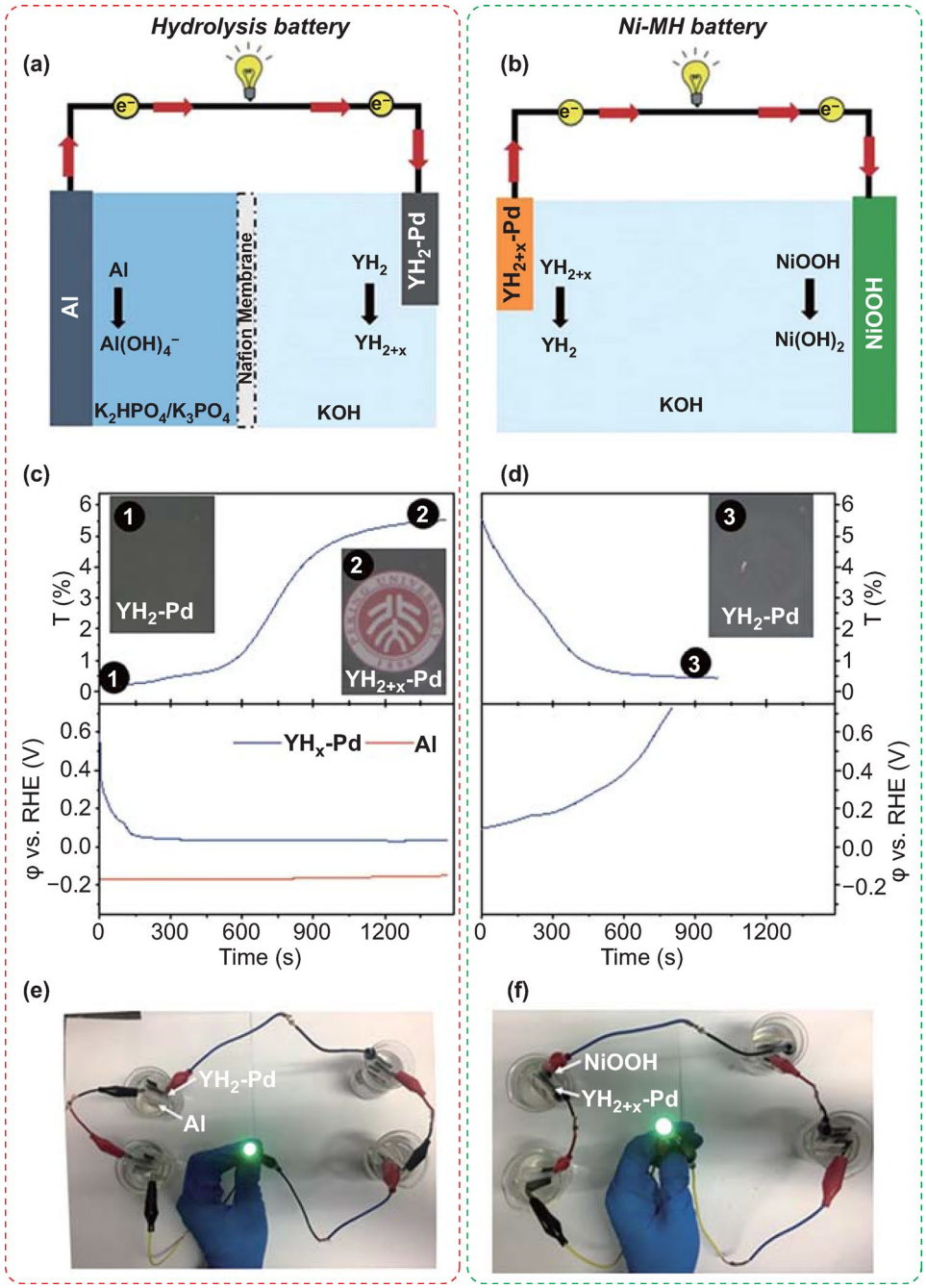

Fig. 13 Schematic illustration of the Al hydrolysis battery **a** and the conventional Ni-MH battery **b** and their operation principle. Synchronized optical transmittance at 500 nm (the upper panel) and potential profiles (the lower panel) of the YH_x-Pd electrode during galvanostatic process in the hydrolysis battery **c** and Ni-MH battery **d**. The current density is 0.2 and 0.05 mA cm^{-2} for the Al hydrolysis battery and the Ni-MH battery, respectively. The potential profile of the Al electrode during the operation of the hydrolysis battery is also shown. Inset: photographs of the YH_x-Pd electrode at different stages as indicated by the corresponding number in the transmittance curve. Photographs of lighting the LED by the Al hydrolysis battery **e** and the MH-Ni battery (**f**). The electrolyte of hydrolysis battery and Ni-MH battery in **e**, **f** is 1 M KOH. Reprinted with permission from Ref. [181]. Copyright 2018 Wiley Online Library

Recently, more attentions were shifted to the preparation and regeneration of $NaBH_4$ for achieving its large-scale practical applications. In the industry of chemical production, $NaBH_4$ is usually synthesized by the Brown–Schlesinger process [184] and the Bayer process [185]. The synthesis

reactions of Schlesinger and Bayer methods are given as follows:

$$4NaH + B(OCH_3)_3 \rightarrow NaBH_4 + 3NaOCH_3 (225 \sim 275\,^{\circ}C) \quad (6)$$

$$Na_2B_4O_7 + 16Na + 8H_2 + 7SiO_2 \rightarrow NaBH_4 + 7Na_2SiO_3 (450 \sim 500\,^{\circ}C) \quad (7)$$

Though the above technologies are mature, they are unsuitable for $NaBH_4$ hydrolysis applications because of the fancy raw materials (Na or NaH) and high-energy consumption processes. Thus, suitable methods for $NaBH_4$ synthesis have been developed with low-cost raw materials instead of sodium or its hydride. MgH_2 was used to react with anhydrous borax ($Na_2B_4O_7$) for $NaBH_4$ synthesis by ball milling method at room temperature (RT). Here, the $NaBH_4$ yield may reach 78% with the addition of Na_2CO_3 [186]. This method introduces not only a novel reducing agent (MgH_2), but also an energy-efficient strategy for $NaBH_4$ synthesis. Enlightened by this, RT ball milling became attractive in $NaBH_4$ synthesis studies, by which Na and MgH_2 could react with B_2O_3 with the $NaBH_4$ yield of ~ 25% [187]. As Na was replaced by safe and cheap NaCl, $NaBH_4$ could also be produced [188]. Subsequently, high-pressure milling was also developed to synthesize $NaBH_4$. For instance, the synthesis of $NaBH_4$ could be achieved by ball milling the hybrid of NaH and MgB_2 under 120 bar H_2 pressure with the yield of ca. 18% [189].

Importantly, considering the sustainability and environmental friendliness, $NaBH_4$ regeneration from $NaBO_2{\cdot}xH_2O$, the hydrolysis by-product, is appealing as the regeneration and hydrolysis form a recycling system. Since Kojima et al. [190] firstly achieved the regeneration of $NaBH_4$ via reacting MgH_2 with $NaBO_2$ under 70 bar H_2 pressure at 550 °C with a ~ 97% yield of $NaBH_4$, $NaBO_2$ has become the main research object for $NaBH_4$ regeneration. Later, the thermochemistry process was substituted by RT ball milling because of high energy consumption under extreme conditions (high reaction temperature and high hydrogen pressure). Hsueh et al. [191–193] adopted MgH_2 to react with anhydrous $NaBO_2$ by ball milling under inert atmosphere. The conversion yields of $NaBH_4$ were > 70%, which indicated that ball milling is advisable for the reaction between MgH_2 and $NaBO_2$. Recently, Ouyang et al. [182, 183, 194] successfully achieved the regeneration of $NaBH_4$ (Fig. 14) by applying the real hydrolysis by-product ($NaBO_2{\cdot}2H_2O$ and $NaBO_2{\cdot}4H_2O$) as raw material with Mg-based reducing agents (Mg, Mg_2Si and $Mg_{17}Al_{12}$) at ambient conditions, where the troublesome heat-wasting process to obtain $NaBO_2$ using a drying procedure at over 350 °C from $NaBO_2{\cdot}xH_2O$ was omitted. The regeneration yield of $NaBH_4$ may reach 78%. Significantly, the charged H^- stored in $NaBH_4$ was completely converted from protonic H^+ in water bound to $NaBO_2$. Particularly, it was found that the regeneration yield of $NaBH_4$ was up ~ 90%, while MgH_2 acted as reducing agent [195]. Recently, Ouyang et al. [196] found that high-energy ball milling of magnesium (Mg) with the mixture of $Na_2B_4O_7{\cdot}xH_2O$ (x = 5, 10) and Na_2CO_3 (obtained by exposing an aqueous solution of $NaBO_2$ to CO_2) resulted in the formation of $NaBH_4$ with a high yield of 80% under ambient conditions. In their approach, after ball milling for just 10 min, only $B_4O_5(OH)_4^{2-}$ was detected (Fig. 15(1)), suggesting that the reaction started with this compound containing two BO_4 tetrahedra and two BO_3 triangles. The B–O bond with a bond length of 1.4418 Å in the BO_4 tetrahedra is weaker than that (1.3683 Å) in the BO_3 triangle. Thus, the B–O bond in the BO_4 tetrahedra preferentially broke via a B–O–Mg–H intermediate, forming B–H and Mg–O (Fig. 15(2, 4)). In the following step, the cleavage of (B)–O–H (O bonded with sp^2 boron) formed the H_2BOH intermediate (Fig. 15(5)), in which B acted as the Lewis acidic site that accepted H^- from MgH_2 leading to the formation of the final products, BH_4^- and MgO. On the other hand, OH^- bonded with sp^3 boron (Fig. 15(3, 4)) was also substituted by H^- from MgH_2, forming BH_4^-. Furthermore, they achieved a higher yield of 93.1% for a short duration (3.5 h) by ball milling hydrated borax ($Na_2B_4O_7{\cdot}10H_2O$ and/or $Na_2B_4O_7{\cdot}5H_2O$) with different reducing agents such as MgH_2, Mg, and NaH under ambient conditions [197]. By replacing the majority of MgH_2 with low-cost Mg, an attractive yield of 78.6% was obtained. These reactions occurred without extra hydrogen gas inputs, meaning the low-cost and sustainable regeneration. More detailed information toward $NaBH_4$ regeneration can be found in a recent review [198].

In the past few years, numerous reports have been published dealing with the regeneration of $NaBH_4$-based spent fuels ($NaBO_2{\cdot}xH_2O$ or $Na_2B_4O_7{\cdot}xH_2O$), whereas the studies upon the regeneration of $LiBH_4$-based spent products were quite limited. Bilen et al. [199] firstly utilized MgH_2 and $LiBO_2$ to synthesize $LiBH_4$ by means of mechano-chemical reaction. Instead of its elements, the hydrolytic product of $LiBH_4$ ($LiBO_2$) was adopted as raw material, which may

© The authors
https://doi.org/10.1007/s40820-021-00657-9

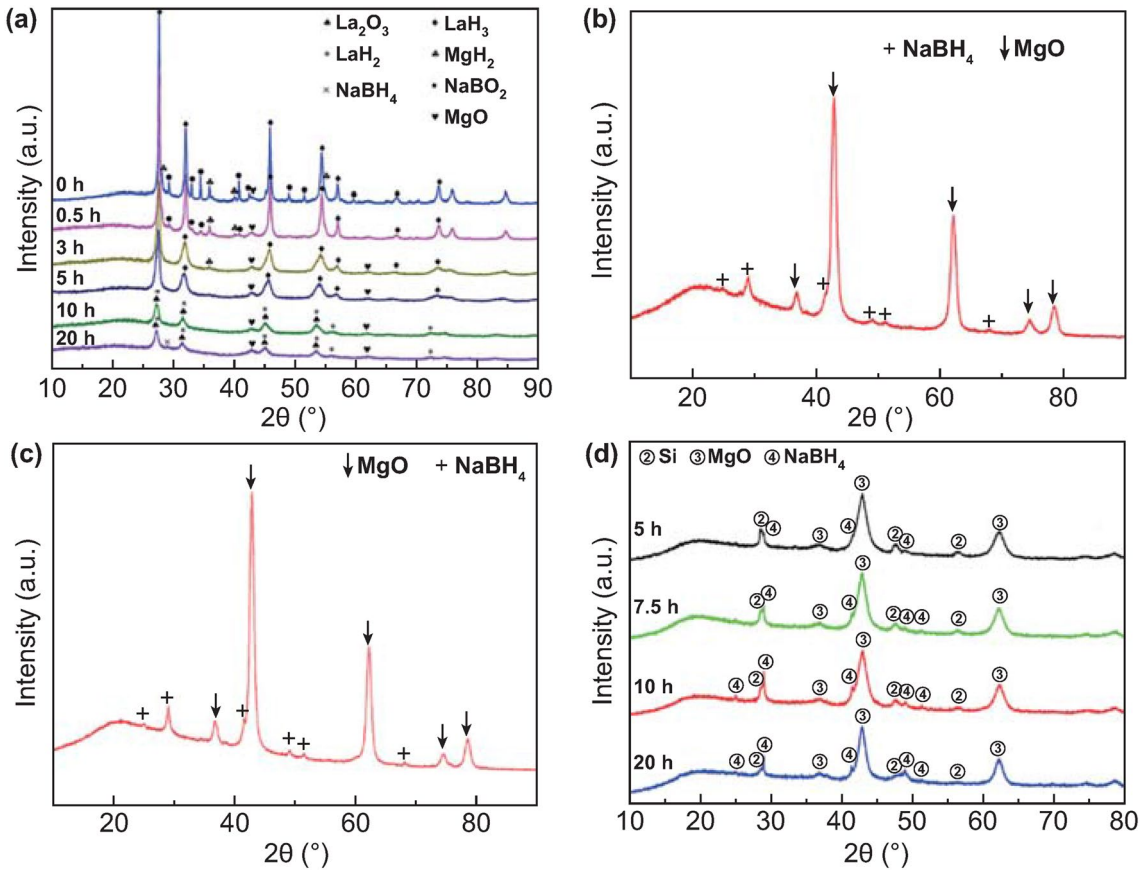

Fig. 14 **a** XRD patterns of the $NaBO_2$–Mg_3La hydride hybrids and the product after ball milling the $NaBO_2$-Mg_3La hydride mixture. **b** XRD pattern of products via ball milling the mixture of $NaBO_2{\cdot}2H_2O$-MgH_2 in 1:5.5 mol ratio for 15 h. **c** XRD curve of products via ball milling the mixture of $NaBO_2{\cdot}2H_2O$-5 Mg for 15 h. **d** XRD spectra of the products after ball milling Mg_2Si and $NaBO_2{\cdot}2H_2O$ mixtures (in 2:1 mol ratio). Reprinted with permission from Ref. [198]. Copyright 2018 MDPI

greatly reduce the application cost of $LiBH_4$ by recycling spent products. However, the tricky heating-wasting process for obtaining anhydrous $LiBO_2$ at elevated temperature (~470 ℃) is inevitable [200]. Stimulated by the successful regeneration of $NaBH_4$, Ouyang et al. [201] reported a facile method to regenerate $LiBH_4$ by ball milling its real hydrolysis by-product ($LiBO_2{\cdot}2H_2O$) with Mg under ambient conditions with a yield of ~40%. This method bypasses

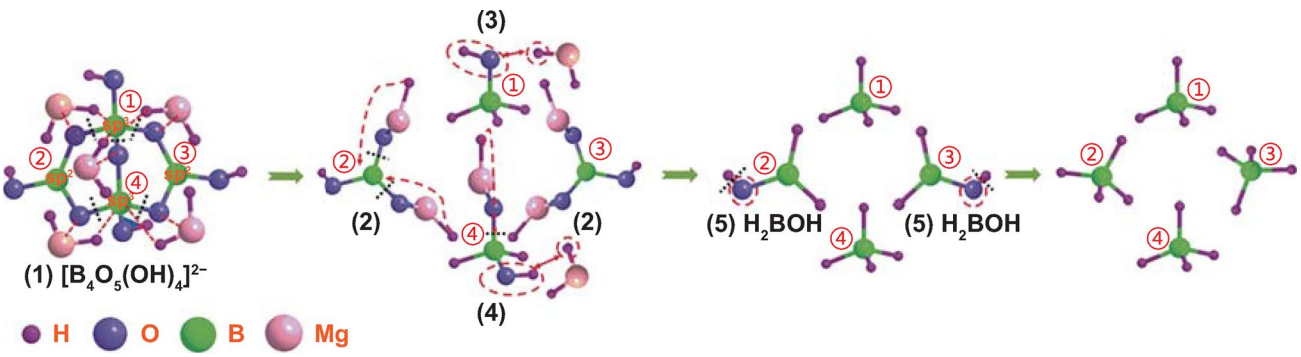

Fig. 15 Proposed reaction mechanism between Mg, Na_2CO_3, and $Na_2B_4O_7{\cdot}10H_2O$ to form $NaBH_4$. Reprinted with permission from Ref. [196]. Copyright 2020 Wiley Online Library

the energy-intensive dehydration procedure to remove water from $LiBO_2{\cdot}2H_2O$ and does not require high-pressure H_2 gas, therefore leading to much reduced costs. Interestingly, it is expected to effectively close the loop of $LiBH_4$ regeneration and hydrolysis, enabling a wide deployment of $LiBH_4$ for hydrogen storage and application. As same as $NaBH_4$ or $LiBH_4$, KBH_4 could also be synthesized by mechanochemical reaction. Bilen et al. [202] successfully synthesized KBH_4 by ball milling KCl, MgH_2, and B_2O_3 in a milling reactor. By tailoring the reactant ratio (MgH_2/KCl) and the milling time, the yield of the reaction reached maximum values, whereas the definite value was not given.

Application of borohydride hydrolysis is limited by limit of their effective regeneration. Though the great achievements have been attained in the regeneration of $NaBH_4$, simplifying synthetic routes and increasing regeneration yield that enable the efficient energy storage and conversion of the "one-pass" hydrogen fuel are two critical targets for large-scale applications. For the anhydrous $NaBO_2$ recycling, it was found that MgH_2 has the best reducing effect. However, its high cost, resulting from the high hydrogenation temperature of Mg, limits the application of such methods. For the direct $NaBH_4$-based spent fuels ($NaBO_2{\cdot}xH_2O$ or $Na_2B_4O_7{\cdot}xH_2O$), they can be reduced to $NaBH_4$ with different reductants (MgH_2, Mg, or Mg_2Si) via ball milling, and the highest yield of $NaBH_4$ may reach 93.1%. Moreover, this process, that uses hydrated metaborate or borax, bypasses the energy-intensive dehydration procedure to obtain anhydrous $NaBO_2$ or $Na_2B_4O_7$ without the requirement of high-pressure H_2 gas; therefore, it could lead to much reduced costs. The boron compounds bound with water may act as hydrogen sources stored in $NaBH_4$ instead of MgH_2. As expected, low-cost waste Al or Al-based alloys may be attractive for achieving the regeneration of $NaBH_4$ via ball milling, enabling a wide deployment of $NaBH_4$ for hydrogen applications. This strategy may provide a new conceptual basis for the development of $LiBH_4$ production or other borohydrides.

4 Conclusions

The present review narrates the recent research progress of hydrogen generation via hydrolysis or alcoholysis by light metal-based materials for potential off- or on-board hydrogen applications, predominantly including borohydrides and Mg-/Al-based materials. The mechanisms of catalytic borohydride hydrolysis and activation of aluminum-based materials via alloying are depicted. Various common methods such as ball milling, catalysis, alloying, and solution modification for improving hydrolysis kinetics are described in detail. In summary, ball milling can refine the particles size to increase reaction activity, but it is unsuitable for practical use in the transportation and storage of the powder. For the hydrolysis of borohydrides, the Co–B-based materials are commonly considered as reactive as noble metals and much more cost-effective. Other metals and Co may form a synergistic effect in Co–B-based ternary or quaternary catalysts. The (catalyzed) hydrolysis of Mg-/Al-based materials has been summarized. The alcoholysis operated at low temperatures can supply hydrogen for special subzero circumstances. The cost is substantially decreased in regeneration of sodium borohydride, making hydrolysis/alcoholysis more practical for on-site hydrogen applications or fuel cells with the advantages of mild operating temperature, environmentally benign by-products, precise controllable of hydrogen release and high-purity H_2. However, the major exothermicity of hydrolysis reactions has not received enough attention, which is even more than the hydrogen energy. The improvement of controllability of hydrolysis helps to design novel on-board hydrogen supply systems.

Acknowledgements This work was financially supported by the National Key R&D Program of China (2018YFB1502101), the Foundation for Innovative Research Groups of the National Natural Science Foundation of China (NSFC51621001), National Natural Science Foundation of China Projects (51771075) and Natural Science Foundation of Guangdong Province of China (2016A030312011). Z.L. acknowledges the funding support from the Australian Research Council (ARC Discovery Projects, DP180102976 and DP210103539).

Open Access This article is licensed under a Creative Commons Attribution 4.0 International License, which permits use, sharing, adaptation, distribution and reproduction in any medium or format, as long as you give appropriate credit to the original author(s) and the source, provide a link to the Creative Commons licence, and indicate if changes were made. The images or other third party material in this article are included in the article's Creative Commons licence, unless indicated otherwise in a credit line to the material. If material is not included in the article's Creative Commons licence and your intended use is not permitted by statutory regulation or exceeds the permitted use, you will need to obtain permission directly from the copyright holder. To view a copy of this licence, visit http://creativecommons.org/licenses/by/4.0/.

References

1. W. Winsche, K.C. Hoffman, F. Salzano, Hydrogen: its future role in the nation's energy economy. Science **180**(4093), 1325–1332 (1973). https://doi.org/10.1126/science.180.4093.1325
2. X.N. Huang, T. Gao, X.L. Pan, D. Wei, C.J. Lv et al., A review: Feasibility of hydrogen generation from the reaction between aluminum and water for fuel cell applications. J. Power Sources **229**, 133–140 (2013). https://doi.org/10.1016/j.jpowsour.2012.12.016
3. S. Ahmed, M. Krumpelt, Hydrogen from hydrocarbon fuels for fuel cells. Int. J. Hydrog. Energy **26**(4), 291–301 (2001). https://doi.org/10.1016/S0360-3199(00)00097-5
4. X. Cheng, Z. Shi, N. Glass, L. Zhang, J. Zhang et al., A review of PEM hydrogen fuel cell contamination: Impacts, mechanisms, and mitigation. J. Power Sources **165**(2), 739–756 (2007). https://doi.org/10.1016/j.jpowsour.2006.12.012
5. L. Schlapbach, A. Zuttel, Hydrogen-storage materials for mobile applications. Nature **414**(6861), 353–358 (2001). https://doi.org/10.1038/35104634
6. A.E. Lutz, R.S. Larson, J.O. Keller, Thermodynamic comparison of fuel cells to the Carnot cycle. Int. J. Hydrog. Energy **27**(10), 1103–1111 (2002). https://doi.org/10.1016/S0360-3199(02)00016-2
7. M.P. Suh, H.J. Park, T.K. Prasad, D.W. Lim, Hydrogen storage in metal-organic frameworks. Chem. Rev. **112**(2), 782–835 (2012). https://doi.org/10.1021/cr200274s
8. U. Eberle, M. Felderhoff, F. Schuth, Chemical and physical solutions for hydrogen storage. Angew. Chem. Int. Ed. **48**(36), 6608–6630 (2009). https://doi.org/10.1002/anie.200806293
9. R. Jain, A. Jain, S. Agarwal, N. Lalla, V. Ganesan et al., Hydrogenation behaviour of Ce-based AB5 intermetallic compounds. J. Alloy Compd. **440**(1–2), 84–88 (2007). https://doi.org/10.1016/j.jallcom.2006.08.326
10. A.W.C. van den Berg, C.O. Areán, Materials for hydrogen-storage: current research trends and perspectives. Chem. Commun. **6**, 668–681 (2008). https://doi.org/10.1039/B712576N
11. N.T. Stetson, Hydrogen storage program area: plenary presentation (US Department of Energy, 2017).
12. A. Yamashita, M. Kondo, S. Goto, N. Ogami, Development of high-pressure hydrogen storage system for the Toyota "Mirai." SAE Technical Paper Series (2015). https://doi.org/10.4271/2015-01-1169
13. M. Aziz, A.T. Wijayanta, A.B.D. Nandiyanto, Ammonia as effective hydrogen storage: a review on production, storage and utilization. Energies **13**(12), 3062 (2020). https://doi.org/10.3390/en13123062
14. M. Felderhoff, C. Weidenthaler, R. von Helmolt, U. Eberle, Hydrogen storage: the remaining scientific and technological challenges. Phys. Chem. Chem. Phys. **9**(21), 2643–2653 (2007). https://doi.org/10.1039/b701563c
15. K. Wang, Z. Pan, X. Yu, Metal B-N-H hydrogen-storage compound: Development and perspectives. J. Alloys Compound. **794**, 303–324 (2019). https://doi.org/10.1016/j.jallcom.2019.04.240
16. N.Z.A.K. Khafidz, Z. Yaakob, K.L. Lim, S.N. Timmiati, The kinetics of lightweight solid-state hydrogen storage materials: A review. Int. J. Hydrog. Energy **41**(30), 13131–13151 (2016). https://doi.org/10.1016/j.ijhydene.2016.05.169
17. A.T. Wijayanta, T. Oda, C.W. Purnomo, T. Kashiwagi, M. Aziz, Liquid hydrogen, methylcyclohexane, and ammonia as potential hydrogen storage: Comparison review. Int. J. Hydrog. Energy **44**(29), 15026–15044 (2019). https://doi.org/10.1016/j.ijhydene.2019.04.112
18. S. Kumar, A. Jain, T. Ichikawa, Y. Kojima, G.K. Dey, Development of vanadium based hydrogen storage material: A review. Renew. Sust. Energ. Rev. **72**, 791–800 (2017). https://doi.org/10.1016/j.rser.2017.01.063
19. A. Jain, R. Jain, S. Agarwal, V. Ganesan, N. Lalla et al., Synthesis, characterization and hydrogenation of ZrFe2-xNix (x= 0.2, 0.4, 0.6, 0.8) alloys. Int. J. Hydrog. Energy **32**(16), 3965–3971 (2007). https://doi.org/10.1016/j.ijhydene.2007.05.001
20. I. Jain, P. Jain, A. Jain, Novel hydrogen storage materials: a review of lightweight complex hydrides. J. Alloy Compd. **503**(2), 303–339 (2010). https://doi.org/10.1016/j.jallcom.2010.04.250
21. A. Jain, E. Kawasako, H. Miyaoka, T. Ma, S. Isobe et al., Destabilization of LiH by Li insertion into Ge. J. Phys. Chem. C **117**(11), 5650–5657 (2013). https://doi.org/10.1021/jp400133t
22. T. Zhang, S. Isobe, A. Jain, Y. Wang, S. Yamaguchi et al., Enhancement of hydrogen desorption kinetics in magnesium hydride by doping with lithium metatitanate. J. Alloy Compd. **711**, 400–405 (2017). https://doi.org/10.1016/j.jallcom.2017.03.361
23. V.A. Yartys, M.V. Lototskyy, E. Akiba, R. Albert, V.E. Antonov et al., Magnesium based materials for hydrogen based energy storage: Past, present and future. Int. J. Hydrog. Energy **44**(15), 7809–7859 (2019). https://doi.org/10.1016/j.ijhydene.2018.12.212
24. M. Jangir, A. Jain, S. Agarwal, T. Zhang, S. Kumar et al., The enhanced de/re-hydrogenation performance of MgH_2 with TiH_2 additive. Int. J. Energ. Res. **42**(3), 1139–1147 (2018). https://doi.org/10.1002/er.3911
25. S. Kumar, A. Jain, H. Miyaoka, T. Ichikawa, Y. Kojima, Catalytic effect of bis (cyclopentadienyl) nickel II on the improvement of the hydrogenation-dehydrogenation of Mg-MgH_2 system. Int. J. Hydrog. Energy **42**(27), 17178–17183 (2017). https://doi.org/10.1016/j.ijhydene.2017.05.090
26. C.W. Hamilton, R.T. Baker, A. Staubitz, I. Manners, B-N compounds for chemical hydrogen storage. Chem. Soc. Rev. **38**(1), 279–293 (2009). https://doi.org/10.1039/B800312M
27. S. Liu, J. Liu, X. Liu, J. Shang, L. Xu et al., Hydrogen storage in incompletely etched multilayer Ti_2CT_x at room

temperature. Nat. Nanotechnol. **16**, 331–336 (2021). https://doi.org/10.1038/s41565-020-00818-8

28. S. Kumar, U. Jain, A. Jain, H. Miyaoka, T. Ichikawa et al., Development of MgLiB based advanced material for onboard hydrogen storage solution. Int. J. Hydrog. Energy **42**(7), 3963–3970 (2017). https://doi.org/10.1016/j.ijhydene.2016.10.061
29. A. Borgschulte, E. Callini, B. Probst, A. Jain, S. Kato et al., Impurity gas analysis of the decomposition of complex hydrides. J. Phys. Chem. C **115**(34), 17220–17226 (2011). https://doi.org/10.1021/jp205566q
30. H. Miyaoka, H. Miyaoka, T. Ichikawa, Y. Kojima, Highly purified hydrogen production from ammonia for PEM fuel cell. Int. J. Hydrog. Energy **43**(31), 14486–14492 (2018). https://doi.org/10.1016/j.ijhydene.2018.06.065
31. K. Eom, E. Cho, H. Kwon, Feasibility of on-board hydrogen production from hydrolysis of Al-Fe alloy for PEMFCs. Int. J. Hydrog. Energy **36**(19), 12338–12342 (2011). https://doi.org/10.1016/j.ijhydene.2011.06.099
32. C. Lang, Y. Jia, X. Yao, Recent advances in liquid-phase chemical hydrogen storage. Energy Storage Mater. **26**, 290–312 (2020). https://doi.org/10.1016/j.ensm.2020.01.010
33. C. Wang, D. Astruc, Recent developments of nanocatalyzed liquid-phase hydrogen generation. Chem. Soc. Rev. **50**, 3437–3484 (2021). https://doi.org/10.1039/D0CS00515K
34. S. Selvaraj, A. Jain, S. Kumar, T. Zhang, S. Isobe et al., Study of cyclic performance of V-Ti-Cr alloys employed for hydrogen compressor. Int. J. Hydrog. Energy **43**(5), 2881–2889 (2018). https://doi.org/10.1016/j.ijhydene.2017.12.159
35. M.H. Grosjean, M. Zidoune, J.Y. Huot, L. Roue, Hydrogen generation via alcoholysis reaction using ball-milled Mg-based materials. Int. J. Hydrog. Energy **31**(9), 1159–1163 (2006). https://doi.org/10.1016/j.ijhydene.2005.10.001
36. M. Wang, L. Ouyang, C. Peng, X. Zhu, W. Zhu et al., Synthesis and hydrolysis of $NaZn(BH_4)_3$ and its ammoniates. J. Mater. Chem. A **5**(32), 17012–17020 (2017). https://doi.org/10.1039/C7TA05082H
37. D.-W. Zhuang, H.-B. Dai, P. Wang, Hydrogen generation from solvolysis of sodium borohydride in ethylene glycol–water mixtures over a wide range of temperature. RSC Adv. **3**(45), 23810 (2013). https://doi.org/10.1039/c3ra43136c
38. M. Ma, L. Ouyang, J. Liu, H. Wang, H. Shao et al., Air-stable hydrogen generation materials and enhanced hydrolysis performance of MgH_2-$LiNH_2$ composites. J. Power Sources **359**, 427–434 (2017). https://doi.org/10.1016/j.jpowsour.2017.05.087
39. S. Kumar, A. Jain, H. Miyaoka, T. Ichikawa, Y. Kojima, Study on the thermal decomposition of $NaBH_4$ catalyzed by $ZrCl_4$. Int. J. Hydrog. Energy **42**(35), 22432–22437 (2017). https://doi.org/10.1016/j.ijhydene.2017.02.060
40. S. Kumar, A. Singh, K. Nakajima, A. Jain, H. Miyaoka et al., Improved hydrogen release from magnesium borohydride by $ZrCl_4$ additive. Int. J. Hydrog. Energy **42**(35), 22342–22347 (2017). https://doi.org/10.1016/j.ijhydene.2016.12.090
41. A. Borgschulte, A. Jain, A.J. Ramirez-Cuesta, P. Martelli, A. Remhof et al., Mobility and dynamics in the complex hydrides $LiAlH_4$ and $LiBH_4$. Faraday Discuss **151**, 213–230 (2011). https://doi.org/10.1039/c0fd00011f
42. V. Kong, Development of hydrogen storage for fuel cellgenerators. i: Hydrogen generation using hydrolysishydrides. Int. J. Hydrog. Energy **24**(7), 665–675 (1999). https://doi.org/10.1016/S0360-3199(98)00113-X
43. M. Nie, Y. Zou, Y. Huang, J. Wang, Ni–Fe–B catalysts for $NaBH_4$ hydrolysis. Int. J. Hydrog. Energy **37**(2), 1568–1576 (2012). https://doi.org/10.1016/j.ijhydene.2011.10.006
44. B. Chen, S.J. Chen, H.A. Bandal, R. Appiah-Ntiamoah, A.R. Jadhav et al., Cobalt nanoparticles supported on magnetic core-shell structured carbon as a highly efficient catalyst for hydrogen generation from $NaBH_4$ hydrolysis. Int. J. Hydrog. Energy **43**(19), 9296–9306 (2018). https://doi.org/10.1016/j.ijhydene.2018.03.193
45. P. Krishnan, T.H. Yang, W.Y. Lee, C.S. Kim, PtRu-$LiCoO_2$ - an efficient catalyst for hydrogen generation from sodium borohydride solutions. J. Power Sources **143**(1–2), 17–23 (2005). https://doi.org/10.1016/j.jpowsour.2004.12.007
46. U.B. Demirci, F. Garin, Kinetics of Ru-promoted sulphated zirconia catalysed hydrogen generation by hydrolysis of sodium tetrahydroborate. J. Mol. Catal. A Chem. **279**(1), 57–62 (2008). https://doi.org/10.1016/j.molcata.2007.09.025
47. H. Inokawa, H. Driss, F. Trovela, H. Miyaoka, T. Ichikawa et al., Catalytic hydrolysis of sodium borohydride on Co catalysts. Int. J. Energ. Res. **40**(15), 2078–2090 (2016). https://doi.org/10.1002/er.3582
48. A.K. Figen, Dehydrogenation characteristics of ammonia borane via boron-based catalysts (Co-B, Ni-B, Cu-B) under different hydrolysis conditions. Int. J. Hydrog. Energy **38**(22), 9186–9197 (2013). https://doi.org/10.1016/j.ijhydene.2013.05.081
49. H.J. Tian, Q.J. Guo, D.Y. Xu, Hydrogen generation from catalytic hydrolysis of alkaline sodium borohydride solution using attapulgite clay-supported Co-B catalyst. J. Power Sources **195**(8), 2136–2142 (2010). https://doi.org/10.1016/j.jpowsour.2009.10.006
50. F. Li, Q. Li, H. Kim, CoB/open-CNTs catalysts for hydrogen generation from alkaline $NaBH_4$ solution. Chem. Eng. J. **210**, 316–324 (2012). https://doi.org/10.1016/j.cej.2012.08.102
51. Y.S. Wei, W. Meng, Y. Wang, Y.X. Gao, K.Z. Qi, K. Zhang, Fast hydrogen generation from $NaBH_4$ hydrolysis catalyzed by nanostructured Co-Ni-B catalysts. Int. J. Hydrog. Energy **42**(9), 6072–6079 (2017). https://doi.org/10.1016/j.ijhydene.2016.11.134
52. Y.C. Lu, M.S. Chen, Y.W. Chen, Hydrogen generation by sodium borohydride hydrolysis on nanosized CoB catalysts supported on TiO_2, Al_2O_3 and CeO_2. Int. J. Hydrog. Energy **37**(5), 4254–4258 (2012). https://doi.org/10.1016/j.ijhydene.2011.11.105
53. E. Marreroalfonso, J. Gray, T. Davis, M. Matthews, Hydrolysis of sodium borohydride with steam. Int. J. Hydrog. Energy

© The authors https://doi.org/10.1007/s40820-021-00657-9

32(18), 4717–4722 (2007). https://doi.org/10.1016/j.ijhydene.2007.07.066

54. A.F. Baye, M.W. Abebe, R. Appiah-Ntiamoah, H. Kim, Engineered iron-carbon-cobalt (Fe_3O_4@C-Co) core-shell composite with synergistic catalytic properties towards hydrogen generation via $NaBH_4$ hydrolysis. J. Colloid Interf. Sci. **543**, 273–284 (2019). https://doi.org/10.1016/j.jcis.2019.02.065
55. K. Holbrook, P. Twist, Hydrolysis of the borohydride ion catalysed by metal–boron alloys. J. Chem. Soci. A: Inorg. Phys. Theor. (1971). https://doi.org/10.1039/J19710000890
56. N. Patel, R. Fernandes, A. Miotello, Promoting effect of transition metal-doped Co-B alloy catalysts for hydrogen production by hydrolysis of alkaline $NaBH_4$ solution. J. Catal. **271**(2), 315–324 (2010). https://doi.org/10.1016/j.jcat.2010.02.014
57. U.B. Demirci, About the Technological Readiness of the H-2 Generation by Hydrolysis of B(-N)-H Compounds. Energy Technol-Ger **6**(3), 470–486 (2018). https://doi.org/10.1002/ente.201700486
58. H.A. Bandal, A.R. Jadhav, H. Kim, Cobalt impregnated magnetite-multiwalled carbon nanotube nanocomposite as magnetically separable efficient catalyst for hydrogen generation by $NaBH_4$ hydrolysis. J. Alloy. Compd. **699**, 1057–1067 (2017). https://doi.org/10.1016/j.jallcom.2016.12.428
59. F. Li, E.E. Arthur, D. La, Q.M. Li, H. Kim, Immobilization of $CoCl_2$ (cobalt chloride) on PAN (polyacrylonitrile) composite nanofiber mesh filled with carbon nanotubes for hydrogen production from hydrolysis of $NaBH_4$ (sodium borohydride). Energy **71**, 32–39 (2014). https://doi.org/10.1016/j.energy.2014.03.130
60. G.R.M. Tomboc, A.H. Tamboli, H. Kim, Synthesis of Co_3O_4 macrocubes catalyst using novel chitosan/urea template for hydrogen generation from sodium borohydride. Energy **121**, 238–245 (2017). https://doi.org/10.1016/j.energy.2017.01.027
61. Y.Y. Huang, K.Y. Wang, L. Cui, W.X. Zhu, A.M. Asiri et al., Effective hydrolysis of sodium borohydride driven by self-supported cobalt oxide nanorod array for on-demand hydrogen generation. Catal. Commun. **87**, 94–97 (2016). https://doi.org/10.1016/j.catcom.2016.09.012
62. M.H. Loghmani, A.F. Shojaei, Hydrogen production through hydrolysis of sodium borohydride: Oleic acid stabilized Co-La-Zr-B nanoparticle as a novel catalyst. Energy **68**, 152–159 (2014). https://doi.org/10.1016/j.energy.2014.02.047
63. F. Seven, N. Sahiner, Enhanced catalytic performance in hydrogen generation from $NaBH_4$ hydrolysis by super porous cryogel supported Co and Ni catalysts. J. Power Sources **272**, 128–136 (2014). https://doi.org/10.1016/j.jpowsour.2014.08.047
64. A.R. Jadhav, H.A. Bandal, H. Kim, $NiCo_2O_4$ hollow sphere as an efficient catalyst for hydrogen generation by $NaBH_4$ hydrolysis. Mater. Lett. **198**, 50–53 (2017). https://doi.org/10.1016/j.matlet.2017.03.161
65. F. Baydaroglu, E. Ozdemir, A. Hasimoglu, An effective synthesis route for improving the catalytic activity of carbon-supported Co-B catalyst for hydrogen generation through hydrolysis of $NaBH_4$. Int. J. Hydrog. Energy **39**(3), 1516–1522 (2014). https://doi.org/10.1016/j.ijhydene.2013.04.111
66. Y.P. Guo, Z.P. Dong, Z.K. Cui, X.J. Zhang, J.T. Ma, Promoting effect of W doped in electrodeposited Co-P catalysts for hydrogen generation from alkaline $NaBH_4$ solution. Int. J. Hydrog. Energy **37**(2), 1577–1583 (2012). https://doi.org/10.1016/j.ijhydene.2011.10.019
67. L.N. Wang, Z. Li, P.P. Zhang, G.X. Wang, G.W. Xie, Hydrogen generation from alkaline $NaBH_4$ solution using Co-Ni-Mo-P/gamma-Al_2O_3 catalysts. Int. J. Hydrog. Energy **41**(3), 1468–1476 (2016). https://doi.org/10.1016/j.ijhydene.2015.11.028
68. Y. Wang, Y. Shen, K.Z. Qi, Z.Q. Cao, K. Zhang et al., Nanostructured cobalt-phosphorous catalysts for hydrogen generation from hydrolysis of sodium borohydride solution. Renew Energ. **89**, 285–294 (2016). https://doi.org/10.1016/j.renene.2015.12.026
69. K. Eom, K. Cho, H. Kwon, Effects of electroless deposition conditions on microstructures of cobalt-phosphorous catalysts and their hydrogen generation properties in alkaline sodium borohydride solution. J. Power Sources **180**(1), 484–490 (2008). https://doi.org/10.1016/j.jpowsour.2008.01.095
70. Y.P. Guo, Q.H. Feng, Z.P. Dong, J.T. Ma, Electrodeposited amorphous Co-P catalyst for hydrogen generation from hydrolysis of alkaline sodium borohydride solution. J. Mol. Catal. A-Chem. **378**, 273–278 (2013). https://doi.org/10.1016/j.molcata.2013.06.018
71. Y. Wang, K.Z. Qi, S.W. Wu, Z.Q. Cao, K. Zhang et al., Preparation, characterization and catalytic sodium borohydride hydrolysis of nanostructured cobalt-phosphorous catalysts. J. Power Sources **284**, 130–137 (2015). https://doi.org/10.1016/j.jpowsour.2015.03.013
72. Y.C. Zhao, Z. Ning, J.N. Tian, H.W. Wang, X.Y. Liang et al., Hydrogen generation by hydrolysis of alkaline $NaBH_4$ solution on Co-Mo-Pd-B amorphous catalyst with efficient catalytic properties. J. Power Sources **207**, 120–126 (2012). https://doi.org/10.1016/j.jpowsour.2012.01.118
73. K. Shimoda, K. Doi, T. Nakagawa, Y. Zhang, H. Miyaoka et al., Comparative study of structural changes in NH_3BH_3, $LiNH_2BH_3$, and KNH_2BH_3 during dehydrogenation process. J. Phys. Chem. C **116**(9), 5957–5964 (2012). https://doi.org/10.1021/jp212351f
74. P.Z. Li, K. Aranishi, Q. Xu, ZIF-8 immobilized nickel nanoparticles: highly effective catalysts for hydrogen generation from hydrolysis of ammonia borane. Chem. Commun. **48**(26), 3173–3175 (2012). https://doi.org/10.1039/c2cc17302f
75. C. Wang, J. Tuninetti, Z. Wang, C. Zhang, R. Ciganda et al., Hydrolysis of ammonia-borane over Ni/ZIF-8 nanocatalyst: high efficiency, mechanism, and controlled hydrogen release. J. Am. Chem. Soc. **139**(33), 11610–11615 (2017). https://doi.org/10.1021/jacs.7b06859
76. Z. Li, T. He, L. Liu, W. Chen, M. Zhang et al., Covalent triazine framework supported non-noble metal nanoparticles with superior activity for catalytic hydrolysis of ammonia

borane: from mechanistic study to catalyst design. Chem. Sci. **8**(1), 781–788 (2017). https://doi.org/10.1039/C6SC02456D

77. F. Fu, C. Wang, Q. Wang, A.M. Martinez-Villacorta, A. Escobar, H. Chong et al., Highly selective and sharp volcano-type synergistic Ni_2Pt@ZIF-8-catalyzed hydrogen evolution from ammonia borane hydrolysis. J. Am. Chem. Soc. **140**(31), 10034–10042 (2018). https://doi.org/10.1021/jacs.8b06511
78. M. Wang, L. Ouyang, M. Zeng, J. Liu, C. Peng et al., Magnesium borohydride hydrolysis with kinetics controlled by ammoniate formation. Int. J. Hydrog. Energy **44**(14), 7392–7401 (2019). https://doi.org/10.1016/j.ijhydene.2019.01.209
79. M.C. Wang, L.Z. Ouyang, J.W. Liu, H. Wang, M. Zhu, Hydrogen generation from sodium borohydride hydrolysis accelerated by zinc chloride without catalyst: A kinetic study. J. Alloy Compd. **717**, 48–54 (2017). https://doi.org/10.1016/j.jallcom.2017.04.274
80. T. Zhang, Y. Wang, T. Song, H. Miyaoka, K. Shinzato et al., Ammonia, a switch for controlling high ionic conductivity in lithium borohydride ammoniates. Joule **2**(8), 1522–1533 (2018). https://doi.org/10.1016/j.joule.2018.04.015
81. M.V. Solovev, O.V. Chashchikhin, P.V. Dorovatovskii, V.N. Khrustalev, A.S. Zyubin et al., Hydrolysis of $Mg(BH_4)(2)$ and its coordination compounds as a way to obtain hydrogen. J. Power Sources **377**, 93–102 (2018). https://doi.org/10.1016/j.jpowsour.2017.11.090
82. J. Chang, H.J. Tian, F.L. Du, Investigation into hydrolysis and alcoholysis of sodium borohydride in ethanol-water solutions in the presence of supported Co-Ce-B catalyst. Int. J. Hydrog. Energy **39**(25), 13087–13097 (2014). https://doi.org/10.1016/j.ijhydene.2014.06.150
83. V.R. Fernandes, A.M.F.R. Pinto, C.M. Rangel, Hydrogen production from sodium borohydride in methanol-water mixtures. Int. J. Hydrog. Energy **35**(18), 9862–9868 (2010). https://doi.org/10.1016/j.ijhydene.2009.11.064
84. J.S. Zhang, T.S. Fisher, J.P. Gore, D. Hazra, P.V. Ramachandran, Heat of reaction measurements of sodium borohydride alcoholysis and hydrolysis. Int. J. Hydrog. Energy **31**(15), 2292–2298 (2006). https://doi.org/10.1016/j.ijhydene.2006.02.026
85. K. Ramya, K.S. Dhathathreyan, J. Sreenivas, S. Kumar, S. Narasimhan, Hydrogen production by alcoholysis of sodium borohydride. Int. J. Energ. Res. **37**(14), 1889–1895 (2013). https://doi.org/10.1002/er.3006
86. L. Zhu, D. Kim, H. Kim, R.I. Masel, M.A. Shannon, Hydrogen generation from hydrides in millimeter scale reactors for micro proton exchange membrane fuel cell applications. J. Power Sources **185**(2), 1334–1339 (2008). https://doi.org/10.1016/j.jpowsour.2008.08.092
87. Y. Kojima, Y. Kawai, M. Kimbara, H. Nakanishi, S. Matsumoto, Hydrogen generation by hydrolysis reaction of lithium borohydride. Int. J. Hydrog. Energy **29**(12), 1213–1217 (2004). https://doi.org/10.1016/j.ijhydene.2003.12.009
88. B. Weng, Z. Wu, Z. Li, H. Yang, H. Leng, Enhanced hydrogen generation by hydrolysis of $LiBH_4$ doped with multiwalled carbon nanotubes for micro proton exchange membrane fuel cell application. J. Power Sources **196**(11), 5095–5101 (2011). https://doi.org/10.1016/j.jpowsour.2011.01.080
89. B. Weng, Z. Wu, Z. Li, H. Yang, Enhanced hydrogen generation from hydrolysis of $LiBH_4$ with diethyl ether addition for micro proton exchange membrane fuel cell application. J. Power Sources **204**, 60–66 (2012). https://doi.org/10.1016/j.jpowsour.2012.01.051
90. B. Weng, Z. Wu, Z. Li, H. Yang, H. Leng, Hydrogen generation from noncatalytic hydrolysis of $LiBH_4/NH_3BH_3$ mixture for fuel cell applications. Int. J. Hydrog. Energy **36**(17), 10870–10876 (2011). https://doi.org/10.1016/j.ijhydene.2011.06.009
91. Y. Kojima, K.-I. Suzuki, Y. Kawai, Hydrogen generation from lithium borohydride solution over nano-sized platinum dispersed on $LiCoO_2$. J. Power Sources **155**(2), 325–328 (2006). https://doi.org/10.1016/j.jpowsour.2005.04.019
92. K. Chen, L.Z. Ouyang, H. Wang, J.W. Liu, H.Y. Shao et al., A high-performance hydrogen generation system: Hydrolysis of $LiBH_4$-based materials catalyzed by transition metal chlorides. Renew. Energy **156**, 655–664 (2020). https://doi.org/10.1016/j.renene.2020.04.030
93. Z.H. Tan, L.Z. Ouyang, J.W. Liu, H. Wang, H.Y. Shao et al., Hydrogen generation by hydrolysis of Mg-Mg_2Si composite and enhanced kinetics performance from introducing of $MgCl_2$ and Si. Int. J. Hydrog. Energy **43**(5), 2903–2912 (2018). https://doi.org/10.1016/j.ijhydene.2017.12.163
94. M. Ma, R. Duan, L. Ouyang, X. Zhu, Z. Chen et al., Hydrogen storage and hydrogen generation properties of $CaMg_2$-based alloys. J. Alloy Compd. **691**, 929–935 (2017). https://doi.org/10.1016/j.jallcom.2016.08.307
95. I. Jain, C. Lal, A. Jain, Hydrogen storage in Mg: a most promising material. Int. J. Hydrog. Energy **35**(10), 5133–5144 (2010). https://doi.org/10.1016/j.ijhydene.2009.08.088
96. M. Grosjean, M. Zidoune, L. Roue, J. Huot, Hydrogen production via hydrolysis reaction from ball-milled Mg-based materials. Int. J. Hydrog. Energy **31**(1), 109–119 (2006). https://doi.org/10.1016/j.ijhydene.2005.01.001
97. J.M. Huang, L.Z. Ouyang, Y.J. Wen, H. Wang, J.W. Liu et al., Improved hydrolysis properties of Mg_3RE hydrides alloyed with Ni. Int. J. Hydrog. Energy **39**(13), 6813–6818 (2014). https://doi.org/10.1016/j.ijhydene.2014.02.155
98. M.H. Huang, L.Z. Ouyang, H. Wang, J.W. Liu, M. Zhu, Hydrogen generation by hydrolysis of MgH_2 and enhanced kinetics performance of ammonium chloride introducing. Int. J. Hydrog. Energy **40**(18), 6145–6150 (2015). https://doi.org/10.1016/j.ijhydene.2015.03.058
99. M. Huang, L. Ouyang, J. Ye, J. Liu, X. Yao et al., Hydrogen generation via hydrolysis of magnesium with seawater using Mo, MoO_2, MoO_3 and MoS_2 as catalysts. J. Mater. Chem. A **5**(18), 8566–8575 (2017). https://doi.org/10.1039/C7TA02457F
100. M.H. Huang, L.Z. Ouyang, J.W. Liu, H. Wang, H.Y. Shao et al., Enhanced hydrogen generation by hydrolysis of Mg doped with flower-like MoS_2 for fuel cell applications. J. Power Sources **365**, 273–281 (2017). https://doi.org/10.1016/j.jpowsour.2017.08.097

© The authors https://doi.org/10.1007/s40820-021-00657-9

101. O.V. Kravchenko, L.G. Sevastyanova, S.A. Urvanov, B.M. Bulychev, Formation of hydrogen from oxidation of Mg, Mg alloys and mixture with Ni Co, Cu and Fe in aqueous salt solutions. Int. J. Hydrog. Energy **39**(11), 5522–5527 (2014). https://doi.org/10.1016/j.ijhydene.2014.01.181
102. L.Z. Ouyang, J.M. Huang, C.J. Fang, Q.A. Zhang, D.L. Sun et al., The controllable hydrolysis rate for $LaMg_{12}$ hydride. Int. J. Hydrog. Energy **37**(17), 12358–12364 (2012). https://doi.org/10.1016/j.ijhydene.2012.05.098
103. L.Z. Ouyang, J.M. Huang, H. Wang, Y.J. Wen et al., Excellent hydrolysis performances of Mg_3RE hydrides. Int. J. Hydrog. Energy **38**(7), 2973–2978 (2013). https://doi.org/10.1016/j.ijhydene.2012.12.092
104. L.Z. Ouyang, J.M. Huang, C.J. Fang, H. Wang, J.W. Liu et al., The high capacity and controllable hydrolysis rate of Mg_3La hydride. J. Alloy Compd. **580**, S317–S319 (2013). https://doi.org/10.1016/j.jallcom.2013.03.153
105. L.Z. Ouyang, Y.J. Xu, H.W. Dong, L.X. Sun, M. Zhu, Production of hydrogen via hydrolysis of hydrides in Mg-La system. Int. J. Hydrog. Energy **34**(24), 9671–9676 (2009). https://doi.org/10.1016/j.ijhydene.2009.09.068
106. J.M. Huang, R.M. Duan, L.Z. Ouyang, Y.J. Wen, H. Wang et al., The effect of particle size on hydrolysis properties of Mg_3La hydrides. Int. J. Hydrog. Energy **39**(25), 13564–13568 (2014). https://doi.org/10.1016/j.ijhydene.2014.04.024
107. M.L. Ma, R.M. Duan, L.Z. Ouyang, X.K. Zhu, C.H. Peng et al., Hydrogen generation via hydrolysis of H-$CaMg_2$ and H-$CaMg_{1.9}Ni_{0.1}$. Int. J. Hydrog. Energy **42**(35), 22312–22317 (2017). https://doi.org/10.1016/j.ijhydene.2017.05.159
108. M. Ma, K. Chen, J. Jiang, X. Yang, H. Wang et al., Enhanced hydrogen generation performance of $CaMg_2$-based materials by ball milling. Inorg. Chem. Front. **7**(4), 918–929 (2020). https://doi.org/10.1039/C9QI01299K
109. M.L. Ma, L.L. Yang, L.Z. Ouyang, H.Y. Shao, M. Zhu, Promoting hydrogen generation from the hydrolysis of Mg-Graphite composites by plasma-assisted milling. Energy **167**, 1205–1211 (2019). https://doi.org/10.1016/j.energy.2018.11.029
110. J. Jiang, L. Ouyang, H. Wang, J. Liu, H. Shao et al., Controllable hydrolysis performance of MgLi alloys and their hydrides. ChemPhysChem **20**(10), 1316–1324 (2019). https://doi.org/10.1002/cphc.201900058
111. M.L. Ma, K. Chen, L.Z. Ouyang, J. Jiang, F. Liu et al., Kinetically controllable hydrogen generation at low temperatures by the alcoholysis of $CaMg_2$-based materials in tailored solutions. Chemsuschem **13**(10), 2709–2718 (2020). https://doi.org/10.1002/cssc.202000089
112. J. Chen, H. Fu, Y.F. Xiong, J.R. Xu, J. Zheng et al., $MgCl_2$ promoted hydrolysis of MgH_2 nanoparticles for highly efficient H-2 generation. Nano Energy **10**, 337–343 (2014). https://doi.org/10.1016/j.nanoen.2014.10.002
113. Z.H. Tan, L.Z. Ouyang, J.M. Huang, J.W. Liu, H. Wang et al., Hydrogen generation via hydrolysis of Mg_2Si. J. Alloy Compd. **770**, 108–115 (2019). https://doi.org/10.1016/j.jallcom.2018.08.122
114. Q. Sun, M.S. Zou, X.Y. Guo, R.J. Yang, H.T. Huang et al., A study of hydrogen generation by reaction of an activated Mg-$CoCl_2$ (magnesium-cobalt chloride) composite with pure water for portable applications. Energy **79**, 310–314 (2015). https://doi.org/10.1016/j.energy.2014.11.016
115. S. Wang, L.X. Sun, F. Xu, C.L. Jiao, J. Zhang et al., Hydrolysis reaction of ball-milled Mg-metal chlorides composite for hydrogen generation for fuel cells. Int. J. Hydrog. Energy **37**(8), 6771–6775 (2012). https://doi.org/10.1016/j.ijhydene.2012.01.099
116. F. Xiao, Y.P. Guo, R.J. Yang, J.M. Li, Hydrogen generation from hydrolysis of activated magnesium/low-melting-point metals alloys. Int. J. Hydrog. Energy **44**(3), 1366–1373 (2019). https://doi.org/10.1016/j.ijhydene.2018.11.165
117. S.L. Li, J.M. Song, J.Y. Uan, Mg-Mg2X (X=Cu, Sn) eutectic alloy for the Mg_2X nano-lamellar compounds to catalyze hydrolysis reaction for H-2 generation and the recycling of pure X metals from the reaction wastes. J. Alloy Compd. **772**, 489–498 (2019). https://doi.org/10.1016/j.jallcom.2018.09.154
118. E. Alasmar, I. Aubert, A. Durand, M. Nakhl, M. Zakhour et al., Hydrogen generation from Mg-$NdNiMg_{15}$ composites by hydrolysis reaction. Int. J. Hydrog. Energy **44**(2), 523–530 (2019). https://doi.org/10.1016/j.ijhydene.2018.10.233
119. A.S. Awad, E. El-Asmar, T. Tayeh, F. Mauvy, M. Nakhl et al., Effect of carbons (G and CFs), TM (Ni, Fe and Al) and oxides (Nb_2O_5 and V_2O_5) on hydrogen generation from ball milled Mg-based hydrolysis reaction for fuel cell. Energy **95**, 175–186 (2016). https://doi.org/10.1016/j.energy.2015.12.004
120. P.P. Liu, H.W. Wu, C.L. Wu, Y.G. Chen, Y.M. Xu et al., Microstructure characteristics and hydrolysis mechanism of Mg-Ca alloy hydrides for hydrogen generation. Int. J. Hydrog. Energy **40**(10), 3806–3812 (2015). https://doi.org/10.1016/j.ijhydene.2015.01.105
121. Y.A. Liu, X.H. Wang, Z.H. Dong, H.Z. Liu, S.Q. Li et al., Hydrogen generation from the hydrolysis of Mg powder ball-milled with $AlCl_3$. Energy **53**, 147–152 (2013). https://doi.org/10.1016/j.energy.2013.01.073
122. X. Hou, Y. Wang, K. Hou, L. Yang, H. Shi et al., Outstanding hydrogen production properties of surface catalysts promoted Mg–Ni–Ce composites at room temperature in simulated seawater. J. Mater. Sci. **55**(30), 14922–14937 (2020). https://doi.org/10.1007/s10853-020-05065-9
123. X. Hou, Y. Wang, Y. Yang, R. Hu, G. Yang et al., Microstructure evolution and controlled hydrolytic hydrogen generation strategy of Mg-rich Mg-Ni-La ternary alloys. Energy **188**, 116081 (2019). https://doi.org/10.1016/j.energy.2019.116081
124. X.J. Hou, Y. Wang, Y.L. Yang, R. Hu, G. Yang et al., Enhanced hydrogen generation behaviors and hydrolysis thermodynamics of as-cast Mg-Ni-Ce magnesium-rich alloys in simulate seawater. Int. J. Hydrog. Energy **44**(44), 24086–24097 (2019). https://doi.org/10.1016/j.ijhydene.2019.07.148
125. X. Hou, Y. Wang, R. Hu, H. Shi, L. Feng et al., Catalytic effect of EG and MoS2 on hydrolysis hydrogen generation behavior of high-energy ball-milled Mg-10wt.%Ni alloys in

NaCl solution—A powerful strategy for superior hydrogen generation performance. Int. J. Energy Res. **43**(14), 8426–8438 (2019). https://doi.org/10.1002/er.4840

126. X. Hou, H. Shi, L. Yang, L. Feng, G. Suo et al., Comparative investigation on feasible hydrolysis H_2 production behavior of commercial Mg-M (M = Ni, Ce, and La) binary alloys modified by high-energy ball milling—Feasible modification strategy for Mg-based hydrogen producing alloys. Int. J. Energy Res. **44**(14), 11956–11972 (2020). https://doi.org/10.1002/er.5843
127. K. Hou, X. Ye, X. Hou, Y. Wang, L. Yang et al., Rapid catalytic hydrolysis performance of Mg alloy enhanced by MoS_2 auxiliary mass transfer. J. Mater. Sci. **56**(7), 4810–4829 (2020). https://doi.org/10.1007/s10853-020-05552-z
128. Y. Nakagawa, C.-H. Lee, K. Matsui, K. Kousaka, S. Isobe et al., Doping effect of Nb species on hydrogen desorption properties of AlH_3. J. Alloy Compd. **734**, 55–59 (2018). https://doi.org/10.1016/j.jallcom.2017.10.273
129. Q.F. Li, N.J. Bjerrum, Aluminum as anode for energy storage and conversion: a review. J. Power Sources **110**(1), 1–10 (2002). https://doi.org/10.1016/S0378-7753(01)01014-X
130. J.S. Bryan, F.B. Krasne, Presynaptic inhibition: the mechanism of protection from habituation of the crayfish lateral giant fibre escape response. J. Physiol. **271**(2), 369–390 (1977). https://doi.org/10.1113/jphysiol.1977.sp012005
131. K. Uehara, H. Takeshita, H. Kotaka, Hydrogen gas generation in the wet cutting of aluminum and its alloys. J. Mater. Process Tech. **127**(2), 174–177 (2002). https://doi.org/10.1016/S0924-0136(02)00121-8
132. Z.Y. Deng, J.M.F. Ferreira, Y. Sakka, Hydrogen-generation materials for portable applications. J. Am. Ceram. Soc. **91**(12), 3825–3834 (2008). https://doi.org/10.1111/j.1551-2916.2008.02800.x
133. H.Z. Wang, D.Y.C. Leung, M.K.H. Leung, M. Ni, A review on hydrogen production using aluminum and aluminum alloys. Renew. Sust. Energ. Rev. **13**(4), 845–853 (2009). https://doi.org/10.1016/j.rser.2008.02.009
134. H.B. Dai, G.L. Ma, H.J. Xia, P. Wang, Reaction of aluminium with alkaline sodium stannate solution as a controlled source of hydrogen. Energy Environ. Sci. **4**(6), 2206–2212 (2011). https://doi.org/10.1039/c1ee00014d
135. G.-L. Ma, H.-B. Dai, D.-W. Zhuang, H.-J. Xia, P. Wang, Controlled hydrogen generation by reaction of aluminum/sodium hydroxide/sodium stannate solid mixture with water. Int. J. Hydrog. Energy **37**(7), 5811–5816 (2012). https://doi.org/10.1016/j.ijhydene.2011.12.157
136. F. Habashi, A short history of hydrometallurgy. Hydrometallurgy **79**(1–2), 15–22 (2005). https://doi.org/10.1016/j.hydromet.2004.01.008
137. J.P. Murray, Aluminum production using high-temperature solar process heat. Sol. Energy **66**(2), 133–142 (1999). https://doi.org/10.1016/S0038-092X(99)00011-0
138. M.Q. Fan, F. Xu, L.X. Sun, Studies on hydrogen generation characteristics of hydrolysis of the ball milling Al-based materials in pure water. Int. J. Hydrog. Energy **32**(14), 2809–2815 (2007). https://doi.org/10.1016/j.ijhydene.2006.12.020
139. M.Q. Fan, L.X. Sun, F. Xu, Hydrogen production for micro-fuel-cell from activated Al-Sn-Zn-X (X: hydride or halide) mixture in water. Renew. Energy **36**(2), 519–524 (2011). https://doi.org/10.1016/j.renene.2010.07.006
140. Y.A. Liu, X.H. Wang, H.Z. Liu, Z.H. Dong, S.Q. Li et al., Effect of salts addition on the hydrogen generation of Al-LiH composite elaborated by ball milling. Energy **89**, 907–913 (2015). https://doi.org/10.1016/j.energy.2015.06.043
141. Y.Y. Jia, J. Shen, H.X. Meng, Y.M. Dong, Y.J. Chai et al., Hydrogen generation using a ball-milled Al/Ni/NaCl mixture. J. Alloy Compd. **588**, 259–264 (2014). https://doi.org/10.1016/j.jallcom.2013.11.058
142. M.Q. Fan, F. Xu, L.X. Sun, Hydrogen generation by hydrolysis reaction of ball-milled Al-Bi alloys. Energy Fuel **21**(4), 2294–2298 (2007). https://doi.org/10.1021/ef0700127
143. X.N. Huang, C.J. Lv, Y.X. Huang, S. Liu, C. Wang et al., Effects of amalgam on hydrogen generation by hydrolysis of aluminum with water. Int. J. Hydrog. Energy **36**(23), 15119–15124 (2011). https://doi.org/10.1016/j.ijhydene.2011.08.073
144. O.V. Kravchenko, K.N. Semenenko, B.M. Bulychev, K.B. Kalmykov, Activation of aluminum metal and its reaction with water. J. Alloy Compd. **397**(1–2), 58–62 (2005). https://doi.org/10.1016/j.jallcom.2004.11.065
145. A.V. Parmuzina, O.V. Kravchenko, Activation of aluminium metal to evolve hydrogen from water. Int. J. Hydrog. Energy **33**(12), 3073–3076 (2008). https://doi.org/10.1016/j.ijhydene.2008.02.025
146. M.Q. Fan, L.X. Sun, F. Xu, Feasibility study of hydrogen production for micro fuel cell from activated Al-In mixture in water. Energy **35**(3), 1333–1337 (2010). https://doi.org/10.1016/j.energy.2009.11.016
147. M.J. Baniamerian, S.E. Moradi, Al-Ga doped nanostructured carbon as a novel material for hydrogen production in water. J. Alloy Compd. **509**(21), 6307–6310 (2011). https://doi.org/10.1016/j.jallcom.2011.03.069
148. J.T. Ziebarth, J.M. Woodall, R.A. Kramer, G. Choi, Liquid phase-enabled reaction of Al-Ga and Al-Ga-In-Sn alloys with water. Int. J. Hydrog. Energy **36**(9), 5271–5279 (2011). https://doi.org/10.1016/j.ijhydene.2011.01.127
149. W. Wang, D.M. Chen, K. Yang, Investigation on microstructure and hydrogen generation performance of Al-rich alloys. Int. J. Hydrog. Energy **35**(21), 12011–12019 (2010). https://doi.org/10.1016/j.ijhydene.2010.08.089
150. T.P. Huang, Q. Gao, D. Liu, S.N. Xu, C.B. Guo et al., Preparation of Al-Ga-In-Sn-Bi quinary alloy and its hydrogen production via water splitting. Int. J. Hydrog. Energy **40**(5), 2354–2362 (2015). https://doi.org/10.1016/j.ijhydene.2014.12.034
151. H.S. Nam, D.J. Srolovitz, Effect of material properties on liquid metal embrittlement in the Al-Ga system. Acta Mater. **57**(5), 1546–1553 (2009). https://doi.org/10.1016/j.actamat.2008.11.041

© The authors https://doi.org/10.1007/s40820-021-00657-9

152. W. Wang, W. Chen, X.M. Zhao, D.M. Chen, K. Yang, Effect of composition on the reactivity of Al-rich alloys with water. Int. J. Hydrog. Energy **37**(24), 18672–18678 (2012). https://doi.org/10.1016/j.ijhydene.2012.09.164
153. S.-C. Tan, H. Gui, X.-H. Yang, B. Yuan, S.-H. Zhan et al., Comparative study on activation of aluminum with four liquid metals to generate hydrogen in alkaline solution. Int. J. Hydrog. Energy **41**(48), 22663–22667 (2016). https://doi.org/10.1016/j.ijhydene.2016.10.090
154. H.H. Wang, Y. Chang, S.J. Dong, Z.F. Lei, Q.B. Zhu et al., Investigation on hydrogen production using multicomponent aluminum alloys at mild conditions and its mechanism. Int. J. Hydrog. Energy **38**(3), 1236–1243 (2013). https://doi.org/10.1016/j.ijhydene.2012.11.034
155. D.X. Qiao, Y.P. Lu, Z.Y. Tang, X.S. Fan, T.M. Wang et al., The superior hydrogen-generation performance of multicomponent Al alloys by the hydrolysis reaction. Int. J. Hydrog. Energy **44**(7), 3527–3537 (2019). https://doi.org/10.1016/j.ijhydene.2018.12.124
156. W. Yang, T. Zhang, J. Zhou, W. Shi, J. Liu et al., Experimental study on the effect of low melting point metal additives on hydrogen production in the aluminum–water reaction. Energy **88**, 537–543 (2015). https://doi.org/10.1016/j.energy.2015.05.069
157. Y. Liu, X. Wang, H. Liu, Z. Dong, S. Li et al., Effect of salts addition on the hydrogen generation of Al–LiH composite elaborated by ball milling. Energy **89**, 907–913 (2015). https://doi.org/10.1016/j.energy.2015.06.043
158. Y. Jia, J. Shen, H. Meng, Y. Dong, Y. Chai et al., Hydrogen generation using a ball-milled Al/Ni/NaCl mixture. J. Alloy. Compd. **588**, 259–264 (2014). https://doi.org/10.1016/j.jallcom.2013.11.058
159. M.-Q. Fan, F. Xu, L.-X. Sun, Hydrogen generation by hydrolysis reaction of ball-milled Al−Bi alloys. Energy Fuels **21**(4), 2294–2298 (2007). https://doi.org/10.1021/ef0700127
160. M.-Q. Fan, L.-X. Sun, F. Xu, Feasibility study of hydrogen production for micro fuel cell from activated Al–In mixture in water. Energy **35**(3), 1333–1337 (2010). https://doi.org/10.1016/j.energy.2009.11.016
161. M.J. Baniamerian, S.E. Moradi, Al–Ga doped nanostructured carbon as a novel material for hydrogen production in water. J. Alloy. Compd. **509**(21), 6307–6310 (2011). https://doi.org/10.1016/j.jallcom.2011.03.069
162. J.T. Ziebarth, J.M. Woodall, R.A. Kramer, G. Choi, Liquid phase-enabled reaction of Al–Ga and Al–Ga–In–Sn alloys with water. Int. J. Hydrog. Energy **36**(9), 5271–5279 (2011). https://doi.org/10.1016/j.ijhydene.2011.01.127
163. C. Wang, C. Qiu, H. Wei, H. Zou, K. Lin et al., Mild hydrogen production from the hydrolysis of Al–Bi–Zn composite powder. Int. J. Hydrog. Energy **46**(14), 9314–9323 (2021). https://doi.org/10.1016/j.ijhydene.2020.12.104
164. M. Su, H. Hu, J. Gan, W. Ye, W. Zhang et al., Thermodynamics, kinetics and reaction mechanism of hydrogen production from a novel Al alloy/NaCl/g-C_3N_4 composite by low temperature hydrolysis. Energy **218**, 119489 (2021). https://doi.org/10.1016/j.energy.2020.119489
165. S. Liu, M.Q. Fan, D. Chen, C.J. Lv, The effect of composition design on the hydrolysis reaction of Al−Li−Sn alloy and water. Energy Sour. Part A: Recov. Util. Environ. Eff. **37**(4), 356–364 (2015). https://doi.org/10.1080/15567036.2011.580325
166. Y. Liu, X. Liu, X. Chen, S. Yang, C. Wang, Hydrogen generation from hydrolysis of activated Al-Bi, Al-Sn powders prepared by gas atomization method. Int. J. Hydrog. Energy **42**(16), 10943–10951 (2017). https://doi.org/10.1016/j.ijhydene.2017.02.205
167. S.P. du Preez, D.G. Bessarabov, Hydrogen generation of mechanochemically activated Al Bi In composites. Int. J. Hydrog. Energy **42**(26), 16589–16602 (2017). https://doi.org/10.1016/j.ijhydene.2017.05.211
168. B.D. Du, W. Wang, W. Chen, D.M. Chen, K. Yang, Grain refinement and Al-water reactivity of Al Ga In Sn alloys. Int. J. Hydrog. Energy **42**(34), 21586–21596 (2017). https://doi.org/10.1016/j.ijhydene.2017.07.105
169. F. Zhang, K. Edalati, M. Arita, Z. Horita, Fast hydrolysis and hydrogen generation on Al-Bi alloys and Al-Bi-C composites synthesized by high-pressure torsion. Int. J. Hydrog. Energy **42**(49), 29121–29130 (2017). https://doi.org/10.1016/j.ijhydene.2017.10.057
170. F. Xu, X. Zhang, L. Sun, F. Yu, P. Li et al., Hydrogen generation of a novel Al $NaMgH_3$ composite reaction with water. Int. J. Hydrog. Energy **42**(52), 30535–30542 (2017). https://doi.org/10.1016/j.ijhydene.2017.10.161
171. C. Zhao, F. Xu, L. Sun, J. Chen, X. Guo et al., A novel Al BiOCl composite for hydrogen generation from water. Int. J. Hydrog. Energy **44**(13), 6655–6662 (2019). https://doi.org/10.1016/j.ijhydene.2018.12.165
172. Z. Liu, H. Zhao, L. Han, W. Cui, L. Zhou et al., Improvement of the acid resistance, catalytic efficiency, and thermostability of nattokinase by multisite-directed mutagenesis. Biotechnol. Bioeng. **116**(8), 1833–1843 (2019). https://doi.org/10.1002/bit.26983
173. X. Guan, Z. Zhou, P. Luo, F. Wu, S. Dong, Hydrogen generation from the reaction of Al-based composites activated by low-melting-point metals/oxides/salts with water. Energy **188**, 116107 (2019). https://doi.org/10.1016/j.energy.2019.116107
174. D. Liu, Q. Gao, Q. An, H. Wang, J. Wei et al., Experimental study on Zn-doped Al-rich alloys for fast on-board hydrogen production. Curr. Comput.-Aided Drug Des. **10**(3), 167 (2020). https://doi.org/10.3390/cryst10030167
175. T. He, W. Chen, W. Wang, F. Ren, H.-R. Stock, Effect of different Cu contents on the microstructure and hydrogen production of Al–Cu-Ga-In-Sn alloys for dissolvable materials. J. Alloy. Compd. **821**, 153489 (2020). https://doi.org/10.1016/j.jallcom.2019.153489
176. T. He, W. Chen, W. Wang, S. Du, S. Deng, Microstructure and hydrogen production of the rapidly solidified Al–Mg-Ga-In-Sn alloy. J. Alloy. Compd. **827**, 154290 (2020). https://doi.org/10.1016/j.jallcom.2020.154290

177. K. Naseem, H. Zhong, H. Wang, L. Ouyang, M. Zhu, Promoting Al hydrolysis via MgH_2 and NaOH addition. J. Alloy. Compd. **831**, 154793 (2020). https://doi.org/10.1016/j.jallcom.2020.154793
178. S. Prabu, H.-W. Wang, Enhanced hydrogen generation from graphite-mixed aluminum hydroxides catalyzed Al/water reaction. Int. J. Hydrog. Energy **45**(58), 33419–33429 (2020). https://doi.org/10.1016/j.ijhydene.2020.09.036
179. J. Guo, Z. Su, J. Tian, J. Deng, T. Fu et al., Enhanced hydrogen generation from Al-water reaction mediated by metal salts. Int. J. Hydrog. Energy **46**(5), 3453–3463 (2021). https://doi.org/10.1016/j.ijhydene.2020.10.220
180. H. Zhong, H. Wang, J.W. Liu, D.L. Sun, F. Fang et al., Enhanced hydrolysis properties and energy efficiency of MgH_2-base hydrides. J. Alloy. Compd. **680**, 419–426 (2016). https://doi.org/10.1016/j.jallcom.2016.04.148
181. R. Xiao, J. Chen, K. Fu, X. Zheng, T. Wang et al., Hydrolysis batteries: generating electrical energy during hydrogen absorption. Angew. Chem. Int. Ed. **57**(8), 2219–2223 (2018). https://doi.org/10.1002/anie.201711666
182. L. Ouyang, W. Chen, J. Liu, M. Felderhoff, H. Wang et al., Enhancing the regeneration process of consumed $NaBH_4$ for hydrogen storage. Adv. Energy Mater. **7**(19), 1700299 (2017). https://doi.org/10.1002/aenm.201700299
183. H. Zhong, L.Z. Ouyang, J.S. Ye, J.W. Liu, H. Wang et al., An one-step approach towards hydrogen production and storage through regeneration of $NaBH_4$. Energy Storage Mater. **7**, 222–228 (2017). https://doi.org/10.1016/j.ensm.2017.03.001
184. H.I. Schlesinger, H.C. Brown, B. Abraham, A. Bond, N. Davidson et al., New developments in the chemistry of diborane and the borohydrides. I. General Summary. J. Am. Chem. Soc. **75**(1), 186–190 (1953). https://doi.org/10.1021/ja01097a049
185. S. Friedrich, L. Konrad, *Production of Alkali Metal Borohydrides*. Google Patents: 1965.
186. Z.P. Li, N. Morigazaki, B.H. Liu, S. Suda, Preparation of sodium borohydride by the reaction of MgH_2 with dehydrated borax through ball milling at room temperature. J. Alloy. Compd. **349**(1–2), 232–236 (2003). https://doi.org/10.1016/S0925-8388(02)00872-1
187. Ç. Çakanyildirim, M. Gürü, The production of $NaBH_4$ from its elements by mechano-chemical reaction and usage in hydrogen recycle. Energy Sour. Part A: Recov. Util. Environ. Eff. **33**(20), 1912–1920 (2011). https://doi.org/10.1080/15567030903503175
188. M. Bilen, M. Gürü, Ç. Çakanyıldırım, Role of NaCl in $NaBH_4$ production and its hydrolysis. Energy Convers. Manag. **72**, 134–140 (2013). https://doi.org/10.1016/j.enconman.2012.08.031
189. S. Garroni, C.B. Minella, D. Pottmaier, C. Pistidda, C. Milanese et al., Mechanochemical synthesis of $NaBH_4$ starting from NaH–MgB_2 reactive hydride composite system. Int. J. Hydrog. Energy **38**(5), 2363–2369 (2013). https://doi.org/10.1016/j.ijhydene.2012.11.136
190. Y. Kojima, T. Haga, Recycling process of sodium metaborate to sodium borohydride. Int. J. Hydrog. Energy **28**(9), 989–993 (2003). https://doi.org/10.1016/S0360-3199(02)00173-8
191. C.-L. Hsueh, C.-H. Liu, B.-H. Chen, C.-Y. Chen, Y.-C. Kuo et al., Regeneration of spent-$NaBH_4$ back to $NaBH_4$ by using high-energy ball milling. Int. J. Hydrog. Energy **34**(4), 1717–1725 (2009). https://doi.org/10.1016/j.ijhydene.2008.12.036
192. L. Kong, X. Cui, H. Jin, J. Wu, H. Du et al., Mechanochemical synthesis of sodium borohydride by recycling sodium metaborate. Energy Fuel **23**(10), 5049–5054 (2009). https://doi.org/10.1021/ef900619y
193. Ç. Çakanyıldırım, M. Gürü, Processing of $NaBH_4$ from $NaBO_2$ with MgH_2 by ball milling and usage as hydrogen carrier. Renew. Energy **35**(9), 1895–1899 (2010). https://doi.org/10.1016/j.renene.2010.01.001
194. M. Felderhoff, L. Ouyang, M. Zhu, H.Z. Zhong, H. Shao et al., Realizing Facile Regeneration of spent $NaBH_4$ with Mg-Al Alloy. J. Mater. Chem. A **7**, 10723–10728 (2019). https://doi.org/10.1039/c9ta00769e
195. W. Chen, L.Z. Ouyang, J.W. Liu, X.D. Yao, H. Wang et al., Hydrolysis and regeneration of sodium borohydride (NaBH4) – A combination of hydrogen production and storage. J. Power Sources **359**, 400–407 (2017). https://doi.org/10.1016/j.jpowsour.2017.05.075
196. Y.Y. Zhu, L.Z. Ouyang, H. Zhong, J.W. Liu, H. Wang et al., Closing the loop for hydrogen storage: facile regeneration of $NaBH_4$ from its hydrolytic product. Angew. Chem. Int. Ed. **59**(22), 8623–8629 (2020). https://doi.org/10.1002/anie.201915988
197. Y. Zhu, L. Ouyang, H. Zhong, J. Liu, H. Wang et al., Efficient synthesis of sodium borohydride: balancing reducing agents with intrinsic hydrogen source in hydrated borax. ACS Sustain. Chem. Eng. **8**(35), 13449–13458 (2020). https://doi.org/10.1021/acssuschemeng.0c04354
198. L. Ouyang, H. Zhong, H.-W. Li, M. Zhu, A recycling hydrogen supply system of $NaBH_4$ based on a facile regeneration process: A review. Inorganics **6**(1), 10 (2018). https://doi.org/10.3390/inorganics6010010
199. M. Bilen, O. Yilmaz, M. Guru, Synthesis of LiBH4 from $LiBO_2$ as hydrogen carrier and its catalytic dehydrogenation. Int. J. Hydrog. Energy **40**(44), 15213–15217 (2015). https://doi.org/10.1016/j.ijhydene.2015.02.085
200. M. Touboul, E. Bétourné, Dehydration process of lithium borates. Solid State Ion. **84**(3), 189–197 (1996). https://doi.org/10.1016/0167-2738(96)00027-6
201. K. Chen, L. Ouyang, H. Zhong, J. Liu, H. Wang et al., Converting H+ from coordinated water into H- enables super facile synthesis of $LiBH_4$. Green Chem. **21**(16), 4380–4387 (2019). https://doi.org/10.1039/C9GC01897B
202. M. Bilen, M. Gürü, Ç. Çakanyildirim, Conversion of KCl into KBH_4 by mechano-chemical reaction and its catalytic decomposition. J. Electron. Mater. **46**(7), 4126–4132 (2017). https://doi.org/10.1007/s11664-017-5340-0

© The authors https://doi.org/10.1007/s40820-021-00657-9